



Calhoun: The NPS Institutional Archive
DSpace Repository

Theses and Dissertations

1. Thesis and Dissertation Collection, all items

1995-03

The effects of low-profile vortex generators on flow in a transonic fan-blade cascade

Gamerdinger, Peter M.

Monterey, California. Naval Postgraduate School

<https://hdl.handle.net/10945/7531>

This publication is a work of the U.S. Government as defined in Title 17, United States Code, Section 101. Copyright protection is not available for this work in the United States.

Downloaded from NPS Archive: Calhoun



Calhoun is the Naval Postgraduate School's public access digital repository for research materials and institutional publications created by the NPS community. Calhoun is named for Professor of Mathematics Guy K. Calhoun, NPS's first appointed -- and published -- scholarly author.

Dudley Knox Library / Naval Postgraduate School
411 Dyer Road / 1 University Circle
Monterey, California USA 93943

<http://www.nps.edu/library>

**NAVAL POSTGRADUATE SCHOOL
MONTEREY, CALIFORNIA**



THESIS

**THE EFFECTS OF LOW-PROFILE
VORTEX GENERATORS
ON FLOW IN A
TRANSONIC FAN-BLADE CASCADE**

by

Peter M. Gamerdinger

March, 1995

Thesis Advisor:

Raymond P. Shreeve

Thesis
G1433

Approved for public release; distribution is unlimited.

DUDLEY KNOX LIBRARY
NAVAL POSTGRADUATE SCHOOL
MONTEREY CA 93943-5101

REPORT DOCUMENTATION PAGE

Form Approved OMB No. 0704-0188

Public reporting burden for this collection of information is estimated to average 1 hour per response, including the time for reviewing instruction, searching existing data sources, gathering and maintaining the data needed, and completing and reviewing the collection of information. Send comments regarding this burden estimate or any other aspect of this collection of information, including suggestions for reducing this burden, to Washington Headquarters Service, Directorate for Information Operations and Reports, 1215 Jefferson Davis Highway, Suite 1204, Arlington, VA 22202-4302, and to the Office of Management and Budget, Paperwork Reduction Project (0704-0188) Washington DC 20503.

1. AGENCY USE ONLY (Leave blank)	2. REPORT DATE March 1995	3. REPORT TYPE AND DATES COVERED Master's Thesis	
4. TITLE AND SUBTITLE THE EFFECTS OF LOW-PROFILE VORTEX GENERATORS ON FLOW IN A TRANSONIC FAN-BLADE CASCADE		5. FUNDING NUMBERS	
6. AUTHOR(S) Peter M. Gamerdinger		8. PERFORMING ORGANIZATION REPORT NUMBER	
7. PERFORMING ORGANIZATION NAME(S) AND ADDRESS(ES) Naval Postgraduate School Monterey CA 93943-5000		10. SPONSORING/MONITORING AGENCY REPORT NUMBER	
9. SPONSORING/MONITORING AGENCY NAME(S) AND ADDRESS(ES)		11. SUPPLEMENTARY NOTES The views expressed in this thesis are those of the author and do not reflect the official policy or position of the Department of Defense or the U.S. Government.	
12a. DISTRIBUTION/AVAILABILITY STATEMENT Approved for public release; distribution is unlimited.		12b. DISTRIBUTION CODE	
13. ABSTRACT (maximum 200 words) Two dimensional fully-mixed-out flow conditions were measured downstream of a two-passage transonic fan-blade cascade which had low-profile vortex generators (VGs) attached to the suction surfaces of the blades. The simulation was conducted using a blow-down wind tunnel at a Mach number of 1.4. The objective was to assess the effects of vortex generating devices on the suction surface shock-boundary layer interaction and the resulting losses. Measurements are reported from tests made with older aluminum blading, with and without VGs, and with a nominally similar new set of steel blading, with and without VGs. Differences between the old and new blading were found to be most significant. While shock structures appeared to be similar with VGs attached, dye injection showed that the shock-induced boundary layer separation was greatly suppressed and the downstream flow was much steadier. With VGs, the flow turning was improved by 0.94 degrees, but the flow loss coefficient increased by about 8%. An extension of the study is needed to fully assess the potential of using low-profile VGs in military fan engines.			
14. SUBJECT TERMS Shock-Boundary Layer Interaction, Vortex Generators, Boundary Layer Separation		15. NUMBER OF PAGES 114	
		16. PRICE CODE	
17. SECURITY CLASSIFICATION OF REPORT Unclassified	18. SECURITY CLASSIFICATION OF THIS PAGE Unclassified	19. SECURITY CLASSIFICATION OF ABSTRACT Unclassified	20. LIMITATION OF ABSTRACT UL

NSN 7540-01-280-5500

Standard Form 298 (Rev. 2-89)
Prescribed by ANSI Std. Z39-18 298-102

Approved for public release; distribution is unlimited.

THE EFFECTS OF LOW-PROFILE VORTEX GENERATORS
ON FLOW IN A TRANSONIC FAN-BLADE CASCADE

Peter M. Gamerding
Lieutenant, United States Navy
B.S., United States Naval Academy, 1983

Submitted in partial fulfillment
of the requirements for the degree of

MASTER OF SCIENCE IN AERONAUTICAL ENGINEERING

from the

NAVAL POSTGRADUATE SCHOOL


March 1995


Author:


Peter M. Gamerding

Approved by:


Raymond P. Shreeve, Thesis Advisor


Garth V. Hobson, Second Reader


Daniel J. Collins, Chairman
Department of Aeronautics and Astronautics

Thesis
G 1433
C. 2

ABSTRACT

Two dimensional fully-mixed-out flow conditions were measured downstream of a two-passage transonic fan-blade cascade which had low-profile vortex generators (VGs) attached to the suction surfaces of the blades. The simulation was conducted using a blow-down wind tunnel at a Mach number of 1.4. The objective was to assess the effects of vortex generating devices on the suction surface shock-boundary layer interaction and the resulting losses. Measurements are reported from tests made with older aluminum blading, with and without VGs, and with a nominally similar new set of steel blading, with and without VGs. Differences between the old and new blading were found to be the most significant. While shock structures appeared to be similar with VGs attached, dye injection showed that the shock-induced boundary layer separation was greatly suppressed and the downstream flow was much steadier. With VGs, the flow turning was improved by 0.94 degrees, but the flow loss coefficient increased by about 8 %. An extension of the study is needed to fully assess the potential of using low-profile VGs in military fan engines.

TABLE OF CONTENTS

I. INTRODUCTION	1
II. EXPERIMENTAL SIMULATION	5
A. TRANSONIC CASCADE MODEL DESCRIPTION	5
B. TEST SECTION INSTRUMENTATION	5
1. Static Pressure Taps	5
2. Vertical Traverse and Impact Probe	9
C. DATA ACQUISITION AND ANALYSIS SYSTEM	10
1. Pressure Measurement System	10
2. Data Acquisition and Reduction Programs	13
D. VISUALIZATION SYSTEMS	14
1. Shadowgraph	14
2. Colored Dye Injection	15
III. EXPERIMENTAL PROGRAM	17
A. ATTACHMENT OF THE VORTEX GENERATORS	17
1. Sizing Based on Boundary Layer Thickness	17
2. Positioning and Attachment	18
B. TEST PROCEDURE	22
C. PROGRAM OF TESTS	23
1. Aluminum Blades Without Vortex Generators	23
2. Aluminum Blades With Vortex Generators	23
3. Steel Blades Without Vortex Generators	24
4. Steel Blades With Vortex Generators	25
IV. RESULTS	
A. DATA COLLECTION AND PRESENTATION	27

B.	ALUMINUM BLADES WITHOUT VORTEX GENERATORS	28
C.	ALUMINUM BLADES WITH VORTEX GENERATORS	31
D.	STEEL BLADES WITHOUT VORTEX GENERATORS	35
E.	STEEL BLADES WITH VORTEX GENERATORS	37
V.	DISCUSSION AND CONCLUSIONS	43
APPENDIX A.	ZOC-14 SOFTWARE USER'S GUIDE	47
APPENDIX B.	MODIFICATIONS TO DATA ACQUISITION PROGRAMS	53
APPENDIX C.	PLACEMENT OF LOW-PROFILE VORTEX GENERATORS	59
APPENDIX D.	REDUCED DATA AND NUMERICAL RESULTS	63
LIST OF REFERENCES		95
INITIAL DISTRIBUTION LIST		97

LIST OF FIGURES

1.	Shock Boundary Layer Interaction	1
2.	Low-Profile Vortex Generator	3
3.	Transonic Wind Tunnel Facility	6
4.	Transonic Wind Tunnel Schematic	7
5.	Test Section Schematic	7
6.	Cascade Blading Geometry	8
7.	Probe Holder Assembly	9
8.	Probe Tip	10
9.	Data Acquisition System Schematic	11
10.	P1 and P2 Operation/Calibration Solenoid Valve	12
11.	P1 and P2 Operation/Calibration Solenoid Valve With Selector Handle	13
12.	Shadowgraph Visualization System	14
13.	Dye Injection Visualization System	15
14.	Polaroid Photograph of Test Section Used to Determine δ	17
15.	Wheeler Doublets Used by McCormick	18
16.	Schematic of Cascade Blade With Vortex Generators Attached	19
17.	Photograph of Middle Blade With Vortex Generators Attached	20
18.	Close-up Photograph of Middle Blade With Vortex Generators Attached	21
19.	Schematic of Dye Injection Ports	24
20.	Reduced Data Example: Aluminum Blades Without VGs, Run 1, 1/18/95	29
21.	Example Pressure Distribution and Fully-Mixed-Out Results: Aluminum Blades Without VGs, Run 1, 1/18/95	30
22.	Example Pressure Distribution: Aluminum Blades With VGs, Run 1, 2/15/95	32
23.	On-Design Shock Positions: Aluminum Blades Without VGs	34
24.	On-Design Shock Positions: Aluminum Blades With VGs	34
25.	Example Pressure Distribution: Steel Blades Without VGs, Run 1, 2/24/95	36
26.	On-Design Shock Positions: Steel Blades With VGs	38

27.	Example Pressure Distribution: Steel Blades With VGs, Run 1, 3/14/95	39
28.	Fully-Mixed-Out Flow Angle (β_3).	41
29.	Fully-Mixed-Out Flow Loss Coefficient (ω_{mixed})	41

LIST OF TABLES

1.	Measured Pressures and Ports Assigned	27
2.	Traversing Probe Survey Positions	28
3.	Wind Tunnel Conditions: Aluminum Blades Without VGs	31
4.	Fully-Mixed-Out Results: Aluminum Blades Without VGs	31
5.	Wind Tunnel Conditions: Aluminum Blades With VGs	33
6.	Fully-Mixed-Out Results: Aluminum Blades With VGs	33
7.	Wind Tunnel Conditions: Steel Blades Without VGs	37
8.	Fully-Mixed-Out Results: Steel Blades Without VGs	37
9.	Wind Tunnel Conditions: Steel Blades With VGs	40
10.	Fully-Mixed-Out Results: Steel Blades With VGs	40
C1.	Boundary Layer Thickness Measurements	59

LIST OF SYMBOLS

P_1	Inlet Static Pressure
P_2	Outlet Static Pressure
P_{REF}	Plenum Stagnation Pressure (Reference Pressure)
C	Chord Length
P_{P1}	Probe Center Port Pressure
P_{P2}	Probe Left Port Pressure
P_{P3}	Probe Right Port Pressure
P_{ATM}	Atmospheric Pressure
P_{STAT}	Calculated static pressure at Probe
T_t	Average Plenum Stagnation Temperature
X_3	Fully-Mixed-Out Dimensionless Velocity
β_3	Fully-Mixed-Out Flow Angle
$\bar{\omega}_{mixed}$	Fully-Mixed-Out Flow Loss Coefficient

ACKNOWLEDGMENTS

I would like to take this opportunity and express my appreciation to those who contributed to the successful completion of this experimental study. I thank Professor Raymond Shreeve for his guidance and the abundance of knowledge he imparted on me, Rick Still for his invaluable assistance and technical expertise, and my wife, Marie, for her patience and support during this seemingly never-ending quest.

I. INTRODUCTION

Increasing supersonic relative inlet Mach numbers are required to meet the demand for higher levels of thrust, while limiting physical size, in turbo fan engines for transonic and supersonic aircraft. The higher Mach numbers lead to stronger shocks which interact with the turbulent boundary layer and adversely affect the total pressure ratio and flow turning angle of the compressor blade row. In a transonic stage, a shock forms in the rotor passage near the blade leading edge and impinges on the suction side boundary layer of the adjacent blade. The resulting flow field is depicted in Figure 1, which displays how the original normal shock branches into two oblique shocks (referred to as the lambda foot) near the blade suction surface. This is due to a region of reversed flow within the shock-boundary layer interaction. If the size of this interaction is large, the reattached boundary layer downstream will be thick. As a result, the design flow turning angles will not be achieved and the flow losses may increase.

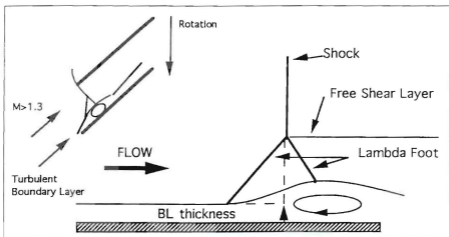


Figure 1. Shock Boundary Layer Interaction (from References 1 and 2)

The process of separation is described, classically, as follows: Viscous shear stresses

remove momentum from the lower region of the boundary layer, and when the low-momentum air flow is subject to an adverse pressure gradient, it is unable to flow against the pressure rise. If the downstream motion near the surface is brought to rest, a back flow is required which creates a region of recirculation and causes the oncoming boundary layer to separate.

In the attached boundary layer, turbulent eddies constantly mix the momentum-rich outer boundary layer fluid with the momentum-poor inner boundary layer fluid. This momentum transport can be augmented using vortex generators (VGs). Such devices shed organized trailing vortices into the boundary layer which act to transfer fluid from the outer to the inner regions, energizing the low momentum fluid near the surface and reducing the likelihood of separation. This mechanism of separation and the beneficial effects of VGs, apply no matter what is the source of adverse pressure gradient. In the present study, the adverse gradient was due to the fan passage shock wave. The particular VGs which were of interest were "low-profile" VGs. Low-profile VGs, described by McCormick [Ref. 3] and United Technologies Research Center (UTRC) [Refs. 1 and 2], produce less parasitic drag than conventional VGs. The VGs used in the present study were one of the designs investigated by UTRC.

Previous experiments [Refs. 1, 2 and 3] examined the effects of low-profile VGs on the shock-boundary layer interaction in a round tube and determined that the shock-induced separation was significantly suppressed and the boundary layer characteristics downstream of the shock were improved. The goal of the present study was to examine the control of the shock-boundary layer interaction in a model simulation of a transonic fan-blade passage flow and determine whether the effects of the VGs were confirmed. The wind tunnel was designed by Demo [Ref. 4] and the original test section geometry was first operated by Hegland [Ref. 5]. The work performed by Collins [Ref. 6] resulted in an operational wind tunnel and cascade test section and the first successful static pressure measurements were made by Golden [Ref. 7]. A traversing, single-port pneumatic probe mechanism was constructed by Myer [Ref. 8] to measure the impact pressure downstream of the fan-blade passages, and Tapp [Ref. 9] demonstrated that periodic conditions could be achieved in the passages by

using a wall bleed system. A three-port pneumatic probe was designed by Austin [Ref. 10] and attached to the existing traversing system to calculate fully-mixed-out conditions in the cascade wake to determine total pressure loss and flow turning angle.

For the current experiments, the original aluminum wind tunnel test section blading was used to repeat and verify the results obtained by Austin [Ref. 10]. Once successful repeatability was accomplished, 6-5-1 low-profile, triangular plow VGs, depicted in Figure 2, were attached to the suction surface of the middle and lower blades to quantify their effect on the total pressure losses and flow turning angle, and to determine the potential benefit of their future use. Concurrent with the wind tunnel testing, a set of nickel-plated, steel blades was manufactured. When the measurements using the VGs were complete, the new blades were installed, and tests to establish the degree of repeatability in the reference configuration, and with VGs attached, were conducted.

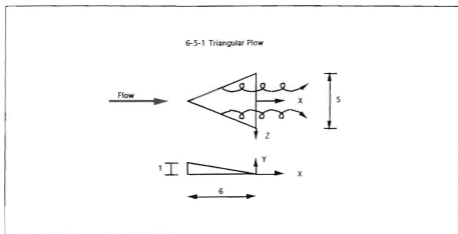


Figure 2. Low-Profile Vortex Generator (from Reference 10)

The results showed that the VGs greatly suppressed the shock-induced boundary layer separation, and the downstream flow was much steadier. It was also determined that the

difference in performance of the old and new blading was significant; the older cascade blades caused decreased flow turning and increased flow losses.

In the present report, the wind tunnel, model simulation, data acquisition system and visualization systems are described in Chapter II. Chapter III describes the experimental program and Chapter IV summarizes the results. A discussion of the results, and the conclusions and recommendations based on the results, are given in Chapter V.

II. EXPERIMENTAL SIMULATION

A. TRANSONIC CASCADE MODEL DESCRIPTION

The transonic cascade wind tunnel was a two-dimensional simulation of the relative flow through a Navy developmental transonic fan at a Mach number of 1.4. The wind tunnel used was a blow-down device located at the Turbopropulsion Laboratory at the Naval Postgraduate School. A schematic of the facility is shown in Figures 3 and 4. The cascade test section, shown in Figure 5, modelled two fan passages using three fan blades. The center blade was a complete blade, while the upper and lower blades modelled only the lower and upper blade surfaces, respectively. The blades were inclined at an incidence angle of 1.15 degrees to the freestream flow at design conditions, and the entire blade geometry is depicted in Figure 6. The inlet pressure to the wind tunnel was controlled by a pneumatically-operated control valve, and a convergent-divergent nozzle provided the resulting Mach 1.4 flow to the test section inlet. The test section back pressure required to simulate fan pressure ratios and position the shocks in the blade passages, was controlled by a three valve system. The back pressure valve (BPV) and back pressure bleed valve (BPPV) were located downstream of the test section and controlled the back pressure of both passages simultaneously. The porous bleed valve (PBV), located on top of the test section, only controlled the pressure in the upper passage. The locations of the valves are shown in Figure 3, and details of their operation are given in References 7 and 9. A full description of the wind tunnel is given in Reference 6.

B. TEST SECTION INSTRUMENTATION

1. Static Pressure Taps

Static pressure taps were located on the test section side plates, the aluminum window (replacement blanks), the lower blade, and the wind tunnel side walls. The pressure taps used for calculating the cascade pressure loss coefficient, looking downstream from above the wind tunnel, were located as follows:

- Inlet static pressure (**P1**): Right side plate, upstream of the blading

- Exit static pressure (P_2): Left side wall, downstream of the blading
- Reference pressure (P_{REF}): Left side wall at the plenum

Golden [Ref. 7] and Tapp [Ref. 9] gave full descriptions with diagrams of the pressure taps and their locations.

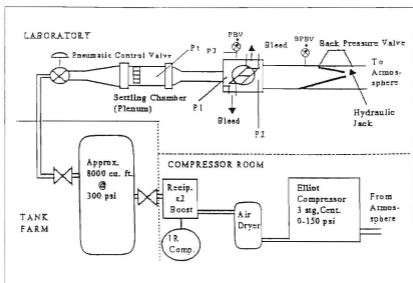


Figure 3. Transonic Wind Tunnel Facility (from Reference 9)

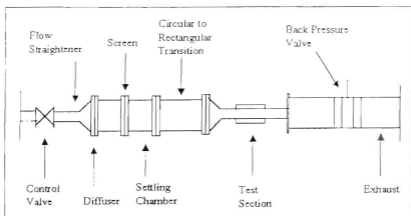


Figure 4. Transonic Wind Tunnel Schematic (from Reference 8)

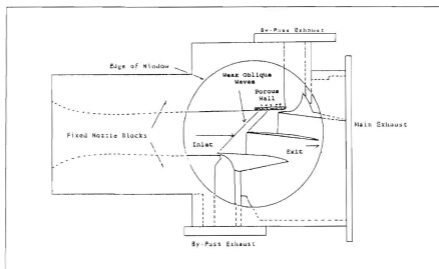


Figure 5. Test Section Schematic (from Reference 7)

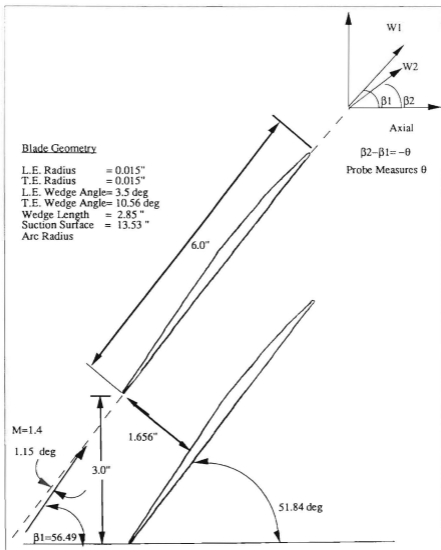


Figure 6. Cascade Blading Geometry (from Reference 10)

2. Vertical Traverse and Impact Probe

The vertical traversing impact probe system was developed by Myre [Ref. 8] for conducting probe surveys downstream of the cascade passages. The impact probe was attached to a probe holder (Figure 7) mounted on a VELMEX UniSlide Motor Driven Assembly. The UniSlide was controlled by a VELMEX NF90 stepping motor controller. The system was designed to accommodate various probe tips, and the one in current use was designed by Austin [Ref. 10] and shown in Figure 8. The 3-hole probe was designed to measure Mach number, flow angle, and velocities in the shear layer as it traversed through the fan-blade wake. The center port was normal to the tunnel air flow and the two outer ports were cut at 40 degree angles horizontally outward. The probe calibration was completed by Austin [Ref. 10], and it was shown that the probe was only sensitive to Mach number and pitch angle.

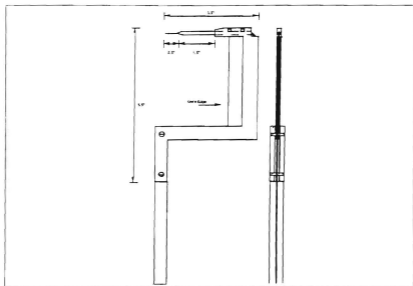


Figure 7. Probe Holder Assembly (from Reference 10)

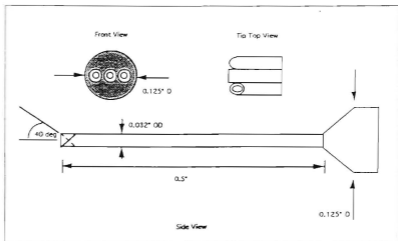


Figure 8. Probe Tip (from Reference 10)

C. DATA ACQUISITION AND ANALYSIS SYSTEM

Wendland [Ref. 11] installed and interfaced the components of the data acquisition and analysis system and wrote the first computer programs for it. Since then, each researcher who has used the transonic wind tunnel system has modified the software to suit the needs of their work. The components of the system were the pressure measurement system and the data acquisition and reduction programs. A schematic of the system is shown in Figure 9, and its operation is outlined in the updated ZOC-14 Software User's Guide, given in Appendix A.

1. Pressure Measurement System

The pressure measurement system is described in Reference 11 and consisted of three sub-systems; namely, a "Zero Operate and Calibrate" (ZOC-14) Data Acquisition System (DAS) for recording pressure data, a continuous static pressure-ratio monitoring system, and the traverse system downstream of the cascade passages. An HP 9000 Series 300 desk top computer acted as the master controller for the ZOC-14 DAS, and also provided the means

for data storage and processing. An HP 6944A multiprogrammer interfaced with the HP 9000 and controlled various ZOC-14 DAS operations and functions. The wind tunnel pressure taps were connected to three Scanivalve ZOC-14 electronic scanning modules which

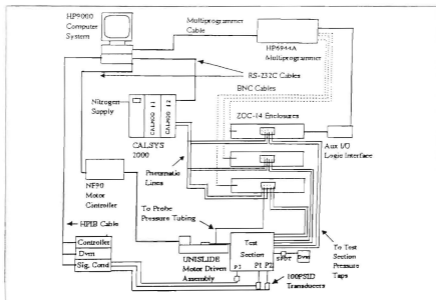


Figure 9. Data Acquisition System Schematic (from Reference 9)

converted the pressures to analog voltage output signals, which were sent to the HP 6944A. Two CALSYS 2000 calibration modules (CALMODs) were incorporated to send reference pressures to the ZOC-14s for calibration purposes. Myre's study only required one ZOC-14 and one CALSYS 2000, but because Wendland's design allowed for expansion, Tapp [Ref. 9] was able to add two ZOC-14s and one CALSYS 2000 for his work. The additional CALSYS 2000 was required due to lower transducer pressure ranges for the new ZOC-14s. The system used in the present study contained all the hardware used by Tapp, but only the one original ZOC-14 (ZOC 1) and the new CALSYS 2000 (CALMOD 2) were used to collect pressure data.

The pressure-ratio monitoring system used two 100 PSID transducers with signal conditioning, an HP 3455A digital voltmeter [Ref. 12], an HP 3497A data acquisition/control unit [Ref. 13], and the HP 9000. Test section inlet and exit static pressures, P_1 and P_2 , and the pressure ratio, P_2/P_1 , set by the tunnel operator, were displayed on the HP 9000 monitor. The pressure ratio was set by the tunnel operator and was used to position the shocks in the cascade passages when the aluminum window blanks were in place and the flow in the test section could not be seen. The readouts were continuous until data acquisition was initiated. To enable a reliable (leak-free) transition between the calibration and operation mode of the 100 PSID transducers, an operation/calibration solenoid valve was installed into the system and is shown in Figures 10 and 11.

The probe traverse system was also programmed through the HP 9000. Details of the system are given by Myre [Ref. 8] and operating procedures are given in References 14 and 15.

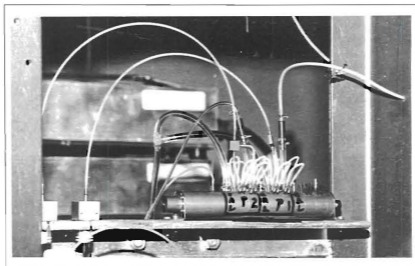


Figure 10. P1 and P2 Operation/Calibration Solenoid Valve

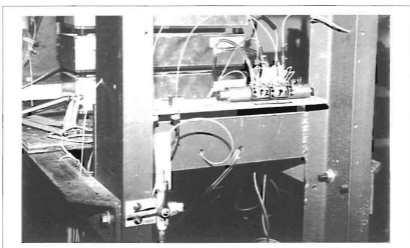


Figure 11. P1 and P2 Operation/Calibration Solenoid Valve With Selector Handle

2. Data Acquisition and Reduction Programs

The original ZOC-14 data acquisition and reduction programs written by Wendland [Ref. 11] were at the core of the wind tunnel software used in the present study. The data acquisition program used herein was "NEW_SCAN_ZOC", which had four different data acquisition options as described in Reference 8. Program "NEW_READ_ZOC1" was the data reduction program, which converted the acquired ZOC-14 voltage data to pressures in psia. The same program was then used to print out and plot the pressures, and calculate the "fully-mixed-out" conditions from probe survey data. The basis for calculating the fully-mixed-out dimensionless velocity, flow angle, and total pressure (downstream of the probe), was that the integrated mass flux measured at the probe station, equalled the passage mass flow rate at the cascade inlet. Due to the probe not traversing parallel to the blade trailing edges, the required blade traverse distance had to be determined. The complete derivation for calculating the fully-mixed-out conditions is given in Reference 16, and Reference 10 contains the equations programmed in "NEW_READ_ZOC1". The programs

"NEW_SCAN_ZOC" and "NEW_READ_ZOC" are listed in References 8 and 10, respectively, and the modifications to these programs which were made during the present work are given in Appendix B.

D. VISUALIZATION SYSTEMS

1. Shadowgraph

A shadowgraph visualization system was used to position, photograph, and video record the shocks in the cascade passages when the test section Plexiglas windows were in place. The system used a continuous light source for visualizing the placement of the shocks and filming with an 8 mm camcorder and monitor system. A spark light source (in the same housing) was used with a polaroid camera and high speed film. To line up the shocks in their on-design position in the upper and lower cascade passages, two vertical, wire guides were attached to one of the test section windows. The shadowgraph system is shown in Figure 12.

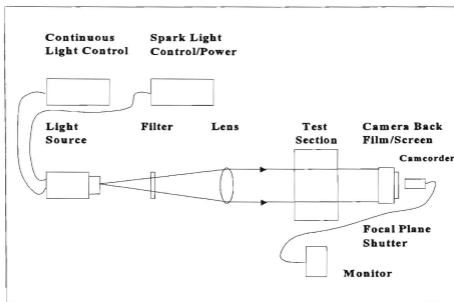


Figure 12. Shadowgraph Visualization System

2. Colored Dye Injection

A colored dye injection visualization system was used to demonstrate the effects the shocks had on the boundary layer separation on the upper surface of the cascade blades. A blue food coloring/alcohol mix was injected into one of the lower blade pressure ports upstream of the shock, and the 8 mm camcorder and monitor system was used to record the event. The injection system is shown schematically in Figure 13.

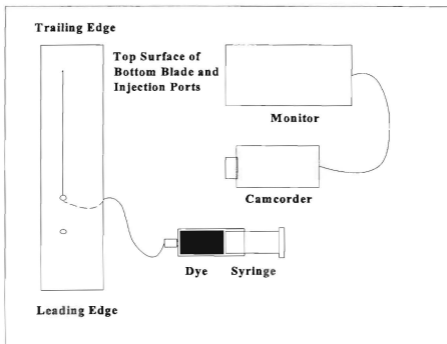


Figure 13. Dye Injection Visualization System

III. EXPERIMENTAL PROGRAM

A. ATTACHMENT OF THE VORTEX GENERATORS

1. Sizing Based on Boundary Layer Thickness

In his study, McCormick [Ref. 3], who used low-profile, wedge-type vortex generators (VGs) which were the invention of Wheeler [Ref. 17], determined that, optimally, the VGs should be between 10-50 % of the boundary layer thickness, δ . Therefore, in the present experiment, in order to use a similar scale, δ had to be determined. A spark shadowgraph photograph of the test section passages, showing the boundary layer forward of the shocks (in the full aft position for clarity) is shown in Figure 14. This photograph was used to determine that $\delta = .064$ inches. Therefore, the (6-5-1) triangular plow VGs (Figure 2) used in the present program, which were 1/32 inch high, had a height (h) = .488 δ . The procedure used for calculating δ is given in Appendix C.

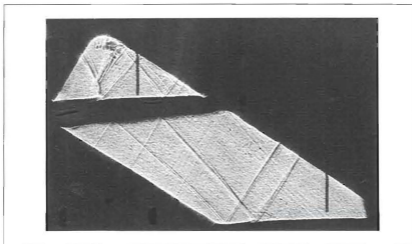


Figure 14. Polaroid Photograph of Test Section Used to Determine δ

2. Positioning and Attachment

In order to be most effective, McCormick [Refs. 3 and 18] found that the VGs had to be positioned $20 \delta - 30 \delta$ forward of the shock position. In his experiments, he used the Wheeler-Doublet arrangement, where two, overlapping rows of the Wheeler wedge-type VGs, spaced at $6.4 h$, were placed across the upper surface of the blade as shown in Figure 15. United Technologies Research Center (UTRC) [Ref. 2] had also completed testing using a single row of both 6-5-1 triangular plow (Figure 2) and triangular ramp low-profile VGs spaced at $6 h$. The ramp had the same geometry as the plow, but the apex was pointed downstream, similar to the Wheeler Doublet. The UTRC results showed that each configuration shed an equal amount of circulation in the wake of the VGs. Villarreal and Tofanel's [Ref. 19] investigation of the drag caused by 6-5-1 triangular plow and ramp VGs showed that the plow created less drag, therefore, the plow configuration with the $6 h$ spacing was used here. Figures 16-18 show how the VGs were positioned on the upper surface of the lower and middle aluminum blades, and Appendix C documents the calculations used to determine those positions and the procedure followed in attaching the VGs to the blades.

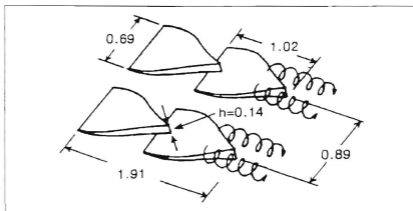


Figure 15. Wheeler-Doublets used by McCormick (from Reference 3)

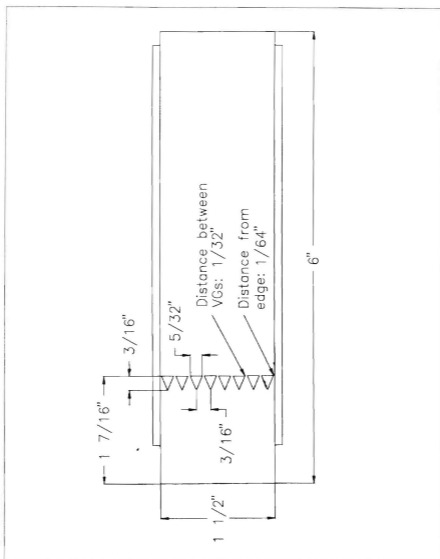


Figure 16. Schematic of Cascade Blade With Vortex Generators Attached

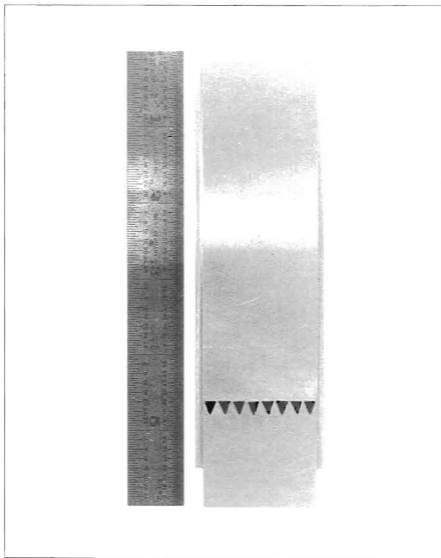


Figure 17. Photograph of Middle Blade With Vortex Generators Attached

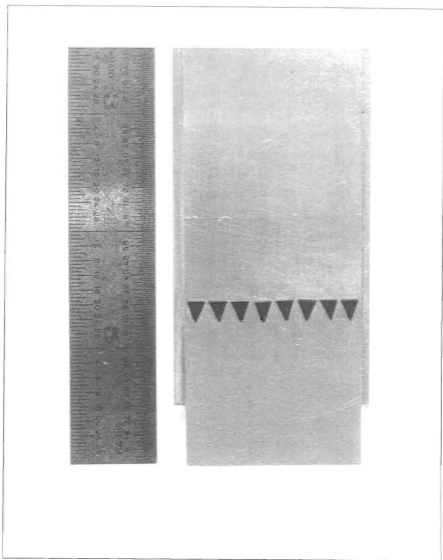


Figure 18. Close-up Photograph of Middle Blade With Vortex Generators Attached

B. TEST PROCEDURE

To ensure that the wind tunnel was operating correctly and that tunnel runs would be repeatable, several initial runs were completed using the shadowgraph system. The purpose of these runs was to familiarize the operator with the wind tunnel operation, and to compare the on-design position of the shocks to that of a file videotape recorded by Tapp [Ref. 9]. Although exact measurements could not be taken due to the unsteadiness of both the upper and lower shocks, the positions, when comparing the relative distances to the guide wires, were very close to the videotape locations. The procedure to set the shocks in their on-design positions in both passages was as follows:

1. The tunnel was allowed to become steady at a plenum pressure of 33 psig.
2. While monitoring the shadowgraph, the BPV was closed by pulling the hydraulic jack handle down four full times.
3. The jack handle was then pulled down smoothly a fifth time until the lower shock moved just aft of the wire guide.
4. The BPBV was then closed until the lower shock moved into position just forward of the wire guide.
5. The PBV was then adjusted to position the upper shock just forward of the wire guide. Closing the PBV (moving handle down) would move the shock forward, and opening it would move the shock aft.

In all past experiments, the BPV and BPBV were reset to full open before each tunnel run, and the above procedure was performed each time. To produce even greater repeatability, tests were completed to determine if the tunnel could be started with the BPV and BPBV in their closed, on-design, positions from the previous tunnel run. If the atmospheric pressure had not changed significantly, and the plenum pressure was again set and allowed to stabilize at 33 psig, the positions of the shocks would be at the on-design locations. If the atmospheric or plenum pressure had varied slightly, the shock positions could be "fine tuned" using the BPBV and PBV. The day's initial tunnel run was always set using the five steps above due to changing atmospheric conditions, but for subsequent runs

on the same day, the procedure using the previous valve settings was used very successfully. When the test conditions were set, in tests in which probe survey data were required, acquisition was initiated at the keyboard of the HP 9000.

C. PROGRAM OF TESTS

1. Aluminum Blades Without Vortex Generators

When it was determined that all the wind tunnel and data acquisition equipment, and the appropriate computer programs and their modifications were operating correctly, a first series of runs was made using the original aluminum cascade blading for comparison with the results obtained by Austin [Ref. 10]. These measurements, including the data for fully-mixed-out conditions, were required to provide a baseline to which measurements with VGs would be referred.

2. Aluminum Blades With Vortex Generators

The second series of runs also used aluminum blading, but the middle blade was replaced with a new aluminum blade, and low-profile VGs were attached to the middle and lower blades. [When the blading was removed from the test section after the first set of runs, the leading edge of the middle blade was found to have eroded significantly due to the mild sand blasting effect of particles in the tunnel air flow. A new aluminum middle blade was available, and it was used to replace the middle blade after VGs had been attached to the suction surface. The upper and lower blades were found not to have deteriorated measurably, and were not replaced.] When data collection and reduction were complete for the second set of runs, the dye injection visualization system was used for comparison with Tapp's [Ref. 9] results. The dye injection ports and shock on-design position are shown in Figure 19. For a direct comparison with Tapp's results, the dye was first injected at $.45 C$ (where C is the blade chord), $.20$ inches aft of the on-design shock position, which was at $.42 C$. The shock was then moved smoothly forward using the BPV until it passed over and moved forward of the dye injection port. A second visualization was carried out using an injection port at $.34 C$, $.46$ inches forward of the on-design shock position. The shock was first positioned at the on-design location, and then the dye was injected to observe the response created as the dye

moved through the shock-boundary layer interaction.

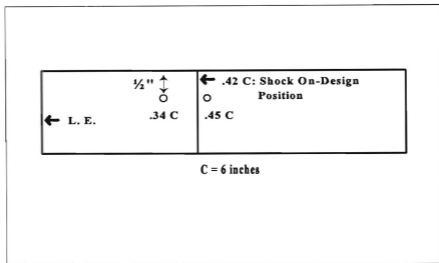


Figure 19. Schematic of Dye Injection Ports

3. Steel Blades Without Vortex Generators

Due to the deterioration apparent in the middle aluminum blade which had been used for the baseline measurements, a third series of tests was conducted using a new set of nickel-plated, steel cascade blading. The new blading was installed without VGs. The blades were "hardened" by nickel plating to better withstand erosion (although the problem was much reduced after the new compressed air system had been used extensively). The results obtained from these runs were to provide an alternate baseline reference to that obtained with the aluminum blades, and to see what degree of repeatability was achieved in similar tests with new hardware. A dye injection visualization using the .34 C injection port was made for comparison with the visualization obtained with VGs installed and with the shock in its on-design position. This mode of visualization was not available on Tapp's [Ref. 9] videotape.

4. Steel Blades With Vortex Generators

The steel blading was removed from the test section, and VGs were attached to the suction surface of the lower and middle blades. A series of tests was conducted to first measure the performance difference between using new blading with and without VGs, and then to assess the performance degradation which results from using old blading. Dye injection visualization using the .34 C injection port was also carried out.

IV. RESULTS

A. DATA COLLECTION AND PRESENTATION

The pressures collected from the three-hole pneumatic probe were P_{p2} , P_{p1} , and P_{p3} , respectively, reading from left to right in Figure 8. All of the measured pressures which were used to calculate the fully-mixed out conditions of the fan-blade wake are listed in Table 1. Table 2 lists the 33 survey positions at which data were taken as the probe traversed downward from its initial position. The data acquisition program "NEW_SCAN_ZOC" was coded to collect 10 pressure samples for each port at each of the survey positions. The raw pressure data were then reduced to pressures and stored on the HP 9000 hard drive for further reduction using the program "NEW_READ_ZOC1". This second program was used to read the reduced pressure data, print it out in tabular form, and plot pressures as a function of the survey position. It also calculated the required blade traverse distance (d_s) for one blade space, the fully-mixed-out dimensionless velocity (X_3), flow angle (β_3), total pressure (P_{t3}), and flow loss coefficient (ζ_{mixed}). The equations used for the calculations are given in Reference 10.

Measured Pressure	ZOC Port Assigned
P_{p1}	32
P_{p2}	24
P_{p3}	25
Atmospheric (P_{ATM})	1
Plenum (P_{REF})	31
Upstream Static (P1)	29
Downstream Static (P2)	30

Table 1. Measured Pressures and Ports Assigned

Position	Distance	Position	Distance	Position	Distance
1	0	12	0.67175	23	1.0155
2	0.09685	13	0.703	24	1.04675
3	0.1937	14	0.73425	25	1.078
4	0.29055	15	0.7655	26	1.10925
5	0.3874	16	0.79675	27	1.1405
6	0.48425	17	0.828	28	1.17175
7	0.5155	18	0.85925	29	1.2686
8	0.54675	19	0.8905	30	1.36545
9	0.578	20	0.92175	31	1.4623
10	0.60925	21	0.953	32	1.55915
11	0.6405	22	0.98425	33	1.656

Table 2. Traversing Probe Survey Positions (inches from start)

B. ALUMINUM BLADES WITHOUT VORTEX GENERATORS

Four tests were completed to ensure repeatability and agreement with the results obtained by Austin [Ref. 10]. Figures 20 and 21 are examples of the pressure data and fully-mixed-out calculations output by "NEW_READ_ZOC1". Tables 3 and 4 summarize the results, and the data for all runs are given in Appendix D. The averages for the atmospheric pressure (P_{ATM}) and total temperature (T_T) are not listed because they were not significant to the results. The atmospheric conditions changed daily, but the conditions set by the tunnel operator, P_{REF} and $P2/P1$, were required to be consistent. The results were very similar to those obtained by Austin [Ref.10], and showed that the repeatability was excellent. The only significant difference, and improvement, was the 2.16 % increase in Pt_3 , which decreased the flow losses by 11.5 %. The shadowgraph system was used to position the shocks in the upper and lower passages, and their locations compared very closely to those observed in Tapp's

[Ref. 9] videotape. Figure 23 shows a polaroid photograph of the shock positions using the spark shadowgraph system.

```

Data Print Out for Doc # 1, Run # 4, File#R151184
Period between samples (sec) 0.00000000000
Sample collection rate (Hz) 100
Number of samples per point 10
Length of data run (sec) 01
The scan type is: 1
Number of scans/traverses: 33
Atmospheric pressure (at) 14.516 psia
Tunnel Pressure Ratio (at) 0.20147061908
    
```

Scan	01	04	08	12	16	20	24
1	5.098	40.588	40.204	15.056	30.725	48.485	46.291
2	5.371	40.373	40.008	15.273	30.727	48.428	46.287
3	5.671	40.372	40.150	15.240	30.744	48.561	46.248
4	5.982	40.477	40.380	15.223	30.744	48.672	46.172
5	5.305	40.206	39.954	15.240	30.719	48.536	45.989
6	5.844	40.407	39.993	15.299	30.692	48.487	46.052
7	5.062	40.502	40.353	15.231	30.692	48.433	46.062
8	5.080	40.511	40.317	15.281	30.658	48.578	46.138
9	4.372	40.174	39.970	15.231	30.589	48.287	45.791
10	4.935	41.482	39.957	15.247	30.546	48.322	44.918
11	4.925	40.377	39.120	15.172	30.520	48.229	43.785
12	4.925	39.193	26.395	15.231	30.443	48.160	42.119
13	4.817	37.275	25.507	15.180	30.486	48.109	39.480
14	4.935	25.313	24.509	15.130	30.460	48.143	37.570
15	4.908	24.839	24.191	15.214	30.589	48.391	36.118
16	4.953	24.865	24.582	15.231	30.512	48.205	36.143
17	4.935	26.394	25.254	15.164	30.443	48.186	38.268
18	4.925	38.761	28.514	15.164	30.460	48.058	41.746
19	4.972	40.836	40.053	15.205	30.443	48.125	44.511
20	4.935	41.526	40.595	15.239	30.469	48.169	45.647
21	4.953	41.664	40.822	15.205	30.426	48.212	45.842
22	4.925	41.759	40.531	15.197	30.452	48.263	45.989
23	4.944	41.829	40.940	15.205	30.512	48.212	45.994
24	4.972	41.742	40.675	15.231	30.460	48.237	45.876
25	4.962	41.573	40.577	15.197	30.434	48.212	45.842
26	4.925	41.664	40.613	15.197	30.452	48.212	45.850
27	4.935	41.530	40.622	15.222	30.452	48.109	45.850
28	4.944	41.530	40.622	15.214	30.477	48.177	45.799
29	4.962	41.561	40.569	15.225	30.469	48.169	45.689
30	4.990	41.327	40.497	15.158	30.323	47.998	45.545
31	4.989	41.284	40.640	15.188	30.374	48.143	45.545
32	4.926	41.232	40.684	15.172	30.408	48.084	45.537
33	4.944	41.258	40.782	15.164	30.409	48.135	45.570

Figure 20. Reduced Data Example: Aluminum Blades Without VGs, Run 1, 1/18/95

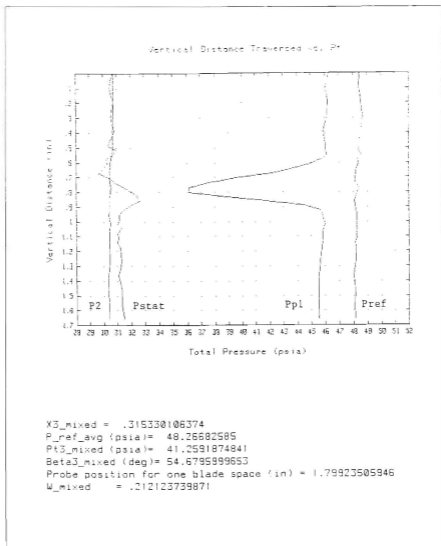


Figure 21. Example Pressure Distribution and Fully-Mixed-Out Results:
Aluminum Blades Without VGs, Run 1, 1/18/95

Run #	P _{ATM} (psia)	T _T (°R)	P _{REF} (psia)	P2/P1
1	14.82	512.0	48.27	2.001
2	14.58	519.5	47.72	1.998
3	14.59	518.0	48.21	1.981
4	14.58	516.5	48.04	2.010
AVERAGE	NA	NA	48.06	1.998
Austin AVG	NA	NA	48.11	2.082
DIFF	NA	NA	-0.105 %	-4.035 %

Table 3. Wind Tunnel Conditions: Aluminum Blades Without VGs

RUN #	X ₃	Pt ₃ (psia)	β ₃ (deg)	ω _{mixed}
1	0.3153	41.26	54.68	0.2121
2	0.3124	40.89	54.78	0.2092
3	0.3131	41.16	54.62	0.2139
4	0.3104	41.04	54.56	0.2130
AVERAGE	0.3128	41.09	54.66	0.2121
Austin AVG	0.3127	40.22	55.00	0.2396
DIFF	+0.032 %	+2.163 %	-0.34 deg	-11.48 %

Table 4. Fully-Mixed-Out Results: Aluminum Blades Without VGs

C. ALUMINUM BLADES WITH VORTEX GENERATORS

The low-profile, triangular plow VGs were attached to the new middle and original lower aluminum blades as described in Appendix C. When the test section was reassembled, four wind tunnel tests were conducted using the shadowgraph system for positioning the shock. Figure 22 shows a representative measured pressure distribution and shows that increased pressure losses were incurred through the cascade. Tables 5 and 6 summarize the results obtained from the four runs, for which the data are given in detail in Appendix D. The

results show that P_{REF} was maintained fairly constant (within 0.104 %), but $P2/P1$ decreased slightly when compared to the reference configuration tests. The increased pressure losses in the cascade wake caused Pt_3 to decrease by 1.51%, leading to an 8.06 % increase in \dot{Q}_{mixed} . The design cascade outlet flow angle was 50 degrees, therefore, the VGs improved β_3 by 0.94 degrees, turning the flow closer to its design value.

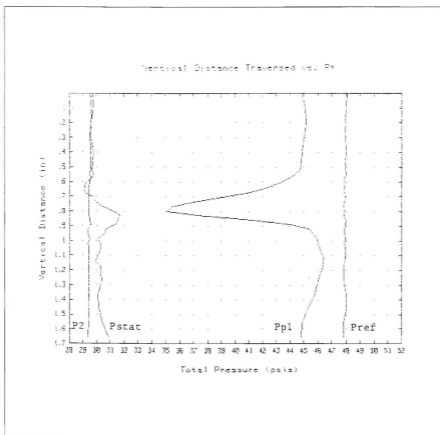


Figure 22. Example Pressure Distribution: Aluminum Blades With VGs, Run 1, 2/15/95

Run #	P _{ATM} (psia)	T _T (°R)	P _{REF} (psia)	P2/P1
1	14.59	516.5	47.92	1.963
2	14.59	512.5	48.18	1.971
3	14.60	510.5	47.96	1.964
4	14.59	511.5	47.99	1.976
AVERAGE	NA	NA	48.01	1.969
AVG W/O	NA	NA	48.06	1.998
DIFF	NA	NA	-0.104 %	-1.451 %

Table 5. Wind Tunnel Conditions: Aluminum Blades With VGs

RUN #	X ₃	Pt ₃ (psia)	β ₃ (deg)	ω _{mixed}
1	0.3214	40.36	53.69	0.2298
2	0.3190	40.64	53.93	0.2281
3	0.3179	40.35	53.59	0.2319
4	0.3175	40.52	53.68	0.2269
AVERAGE	0.3190	40.47	53.72	0.2292
AVG W/O	0.3128	41.09	54.66	0.2121
DIFF	+1.982 %	-1.509 %	-0.94 deg	+8.062 %

Table 6. Fully-Mixed-Out Results: Aluminum Blades With VGs

Additional tests were conducted, and 8mm videotapes were made of the shock structure seen on the shadowgraph screen and of the dye injection patterns. Polaroid photographs were also taken of the shock structure using the spark light source. The shadowgraph showed that the shock locations were slightly further upstream (more forward of the guide wires), and the lambda foot was more curved, but less well defined in the lower passage than when the VGs were not installed. Figures 23 and 24 provide a comparison

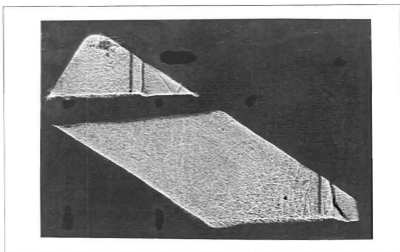


Figure 23. On-Design Shock Positions: Aluminum Blades Without VGs

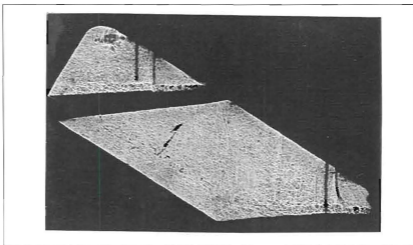


Figure 24. On-Design Shock Positions: Aluminum Blades With VGs

between the two shock structures. The first dye injection was at the .45 C position. The shock was moved forward (by increasing the back pressure) from the full aft position, passed the injection point. When compared to Tapp's [Ref. 9] videotape, less boundary layer separation (sideways and upstream spreading) was observed. The second dye injection was made at the .34 C position with the shock stationary at its on-design location. There was a small amount of separation, evidenced by spreading on the surface under the shock, however, the jet of injectant generally appeared to "bloom" as it passed through the shock and moved downstream. When the back pressure was raised to move the shock forward across the injection port, the spreading on the surface increased somewhat, until the shock passed.

D. STEEL BLADES WITHOUT VORTEX GENERATORS

New steel blades were installed in place of the aluminum blades in the test section and four wind tunnel tests were completed to obtain probe survey data. Figure 25 shows an example of the measured pressure distribution, and Tables 7 and 8 summarize and compare the reduced data. Complete data for all four runs are given in Appendix D. Additional tests were conducted for flow visualization. The shadowgraph system was again used, and an 8mm videotape was recorded to compare with Tapp's [Ref. 9] observations. The shock positions, structure, and behavior as the shock was moved forward through the passage, were observed to be virtually identical to Tapp's results. A dye injection test, using the .34 C injection port, with the shocks in their on-design positions, was also conducted for comparison with the observations made with VGs installed. The interaction at the shock was very significant, with the dye being spread across the entire width of the blade, downstream, and to both sides. After sufficient time for observation, the shock was moved forward (by increasing the back pressure) until it passed over the injection port. The flow separation increased greatly, even spraying dye up onto the Plexiglas windows. This behavior contrasted graphically with what had been observed with the aluminum blades when the VGs were installed.

The probe survey results in Tables 7 and 8 show that the steel blading performed better, in every respect, than the older aluminum blades. A slightly higher pressure ratio was

attained, and less overall loss occurred in the passage. The downstream flow angle also improved to within 3 degrees of the design value. The improvement was possibly attributable to the degradation of the aluminum blades, which had visible roughness on all leading edges and surfaces, especially the middle blade.

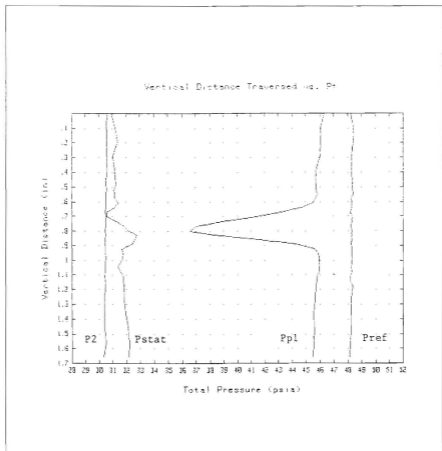


Figure 25. Example Pressure Distribution: Steel Blades Without VGs, Run 1, 2/24/95

Run #	P _{ATM} (psia)	T _T (°R)	P _{REF} (psia)	P2/P1
1	14.79	515.0	48.27	2.005
2	14.79	515.0	48.04	2.019
3	14.77	514.5	48.33	2.001
4	14.78	513.5	47.78	2.011
AVERAGE	NA	NA	48.11	2.009
AI W/O VGs	NA	NA	48.06	1.998
DIFF	NA	NA	+0.104 %	+0.551 %

Table 7. Wind Tunnel Conditions: Steel Blades Without VGs

RUN #	X ₃	P _t (psia)	β ₃ (deg)	ω _{mixed}
1	0.3079	41.35	52.83	0.2098
2	0.3058	41.15	52.83	0.2097
3	0.3110	41.44	52.60	0.2085
4	0.3055	41.01	52.94	0.2069
AVERAGE	0.3076	41.24	52.80	0.2087
AI W/O VGs	0.3128	41.09	54.66	0.2121
DIFF	-1.662 %	+0.365 %	-1.86 deg	-1.603 %

Table 8. Fully-Mixed-Out Results: Steel Blades Without VGs

E. STEEL BLADES WITH VORTEX GENERATORS

The low-profile VGs were attached to the middle and lower steel blades, and four tests were completed for comparison with the configuration without VGs attached, and to determine if increased flow turning and decreased flow separation would result. A fifth test using dye injection at the .34 C injection port, with the shocks in their on-design position, was conducted for comparison with the observations made with the aluminum blades with VGs,

and the steel blades without VGs. The dye injection showed less boundary layer separation at the shock when compared to the steel blades without VGs, but showed a slight increase in blooming when compared to the aluminum blades with VGs.

During the tests, the shadowgraph showed that the shock structures were similar to those that developed on the aluminum blades with VGs attached. The difference was that the oblique shocks on the lower blade were sharper, and more defined, than the shocks on the lower aluminum blade. Figure 26 shows the shock structures, and can be compared to Figure 24 (Aluminum blades with VGs).

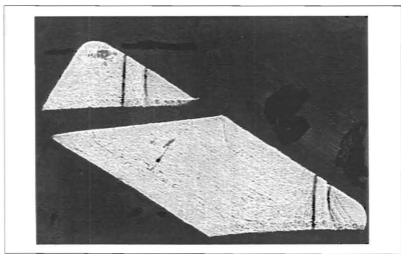


Figure 26. On-Design Shock Position: Steel Blades With VGs

Figure 27 shows an example of the measured pressure distribution, and Tables 9 and 10 summarize and compare the reduced data. Complete data for all four tests are given in Appendix D. The results show that the pressure ratio, flow angle, and flow losses all increased. For this final series of tests, P_2 was measured from a static port on the other side of the test section, directly across from the original port. This was done because of clogging in the original port from the previous dye injection tests, and is the most probable reason for

the increase in pressure ratio. **P2** was not used in the calculation of flow angle or flow loss, and therefore, has no effect on these performance measurements. The 7.09 % increase in flow losses was very comparable to the losses incurred when VGs were attached to the aluminum blades, where an 8.06 % increase was measured. The increase in flow angle, signifying less flow turning, was not expected based on the experience with the aluminum blading. However, the new steel blades, with their new polished finish, had already improved the flow turning by 1.86 degrees, which was quite significant. This may be the best performance which can be achieved by this blading geometry. The attachment of VGs therefore had adversely affected the performance. Figures 28 and 29 summarize the flow angle and flow loss results from all four blading configurations.

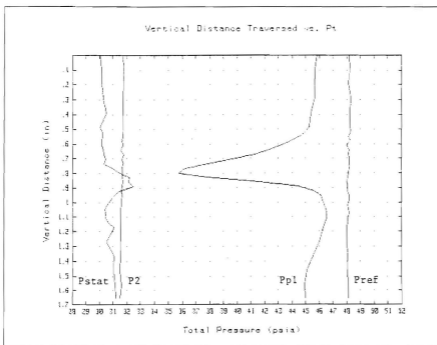


Figure 27. Example Pressure Distribution: Steel Blades With VGs, Run 1, 3/14/95

Run #	P_{ATM} (psia)	T_T ($^{\circ}R$)	P_{REF} (psia)	P2/P1
1	14.80	520.0	48.13	2.079
2	14.80	519.5	49.16	2.070
3	14.81	520.0	48.27	2.081
4	14.81	523.0	48.12	2.066
AVERAGE	NA	NA	48.42	2.074
W/O VGs	NA	NA	48.11	2.009
DIFF	NA	NA	+0.639 %	+3.235 %

Table 9. Wind Tunnel Conditions: Steel Blades With VGs

RUN #	X_3	Pt_3 (psia)	β_3 (deg)	ω_{mixed}
1	0.3159	40.72	54.20	0.2256
2	0.3183	41.61	54.09	0.2249
3	0.3167	40.88	54.00	0.2237
4	0.3186	40.91	53.90	0.2199
AVERAGE	0.3174	41.03	54.05	0.2235
W/O VGs	0.3076	41.24	52.80	0.2087
DIFF	+3.186 %	-0.509 %	+1.25 deg	+7.092 %

Table 10. Fully-Mixed-Out Results: Steel Blades With VGs

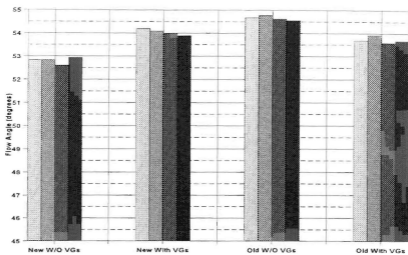


Figure 28. Fully-Mixed-Out Flow Angle (β_s)

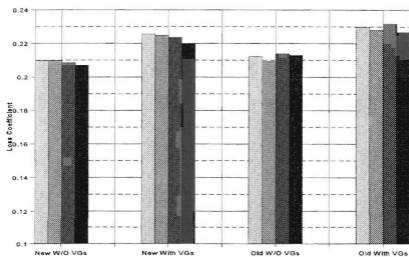


Figure 29. Fully-Mixed-Out Flow Loss Coefficient (ω_{mixed})

V. DISCUSSION AND CONCLUSIONS

The dye injection results, which showed that the extent of shock-induced separation decreased when VGs were attached to the cascade blading are in concurrence with McCormick [Ref. 3], who also found that low-profile VGs suppressed the separation and improved the boundary layer characteristics downstream of the shock. McCormick also observed that the lower mass-averaged total pressure in the wake of the interaction results from suppression of the separation bubble, which decreases the extent of the total pressure region associated with passage through the lambda foot shock system, and increases the extent of the normal shock.

The degradation in transonic blading performance as a result of blade deterioration and roughness has been measured in transonic rotor tests and reported in a recent paper by Suder et al [Ref. 20]. The results obtained in the present cascade study, which showed that older, rougher, and slightly eroded blading adversely affected flow turning and flow loss, are consistent with the rotor results of Suder et al.

The last set of tests showed that flow turning was not improved when VGs were attached to the new set of steel blades. This was not consistent with the tests using the older, aluminum blading. The effect on flow turning when using the new blading without VGs, was twice the improvement which resulted when the older blading, with VGs attached, was used. This large increase in flow turning was possibly the best which could be achieved with the geometry, and any alterations to the configuration, including adding VGs, would have adverse results.

A summary of the conclusions drawn from the present study is as follows:

- Low-profile vortex generators:
 - * reduced shock-induced boundary layer separation
 - * increased flow turning when old blading was used
 - * decreased flow turning when new blading was used
 - * decreased fully-mixed-out total pressure
 - * increased fully-mixed-out flow loss

- Roughness and erosion:
 - decreased flow turning
 - decreased fully-mixed-out total pressure
 - increased fully-mixed-out flow loss

It is recommended that additional experiments be conducted using the same four test programs used in the present study, but instead of attaching the low-profile VGs in the triangular plow configuration, triangular ramps should be investigated. The UTRC studies concluded that the plow configuration initially de-energized the boundary layer just downstream of the VGs before it increased the momentum transport further downstream [Ref. 2]. The strength of the vortices grew to the same magnitude as those produced by the triangular ramps, but because there was no initial de-energization when the ramps were used, this configuration should be tried.

The pressure distribution plots for both sets of blading without VGs attached show that the total pressure (P_{p1}) measured by the impact probe downstream of the middle blade pressure and suction surfaces were virtually a mirror image of each other. The plots with VGs attached show a pressure distribution downstream of the pressure surface which had higher values, indicating less flow losses, and was not similar in shape to the distribution downstream of the suction surface. This difference was probably due to waves from the leading edges of the triangular plows on the lower blade. Therefore, tests using the ramp configuration (the waves from the leading edges will be different) are again suggested for comparison.

In the present study, the VGs were placed at a distance of 20δ upstream of the on-design shock position. Future experiments should investigate the performance obtained when the VGs are attached at a distance of 30δ upstream of the shock position in both the plow and ramp configuration. This will show a performance comparison at the two low-profile VG effective range limits which were determined by McCormick [Ref. 3].

Experiments using smaller VGs would be desirable, because the height (h) of the current VGs, for the measured boundary layer thickness (δ), are at the upper limit

recommended by McCormick [Ref. 3]. Dye injection tests with the video camera on a level plane with the lower blades would also be beneficial in determining the vertical blooming of the shock-induced boundary layer separation.

APPENDIX A. ZOC-14 SOFTWARE USER'S GUIDE

The original operating guide was written by Myre [Ref. 7], updated by Tapp [Ref. 8] after a second CALSYS2000 calibration module was added, and was further modified during the present study to reflect the current tunnel operation.

1. START-UP

- Turn on the HP 6944A, CALSYS 2000 CALMODS #1 and #2, ZOC-14 Enclosures #1, #2 and #3, HP 3497A, HP 3455A and HP 9000. (Program "SYS_ZOC" will boot)
- From the "HP 9000 Series 300 Computer Data Acquisition/Reduction System Menu", Press F7, "Set Time and Date". Update as necessary.
- Press F2, "Scan ZOC System", to enter "HP Multi-Programmer (HP 6944A) Operation Menu".

2. CALMOD #1 AND #2 INITIALIZATION

NOTE: CALMOD #1 and #2 initialization should always be completed prior to a day's tunnel runs and after any files have been manipulated.

- Press F1, "ZOC-14 Modules Menu", to load program "ZOC_MENU" and enter "ZOC Electronic Pressure Module Operation Menu".
- Press F4, "Read CALSYS 2000 calibration pressures". Type 1 and "return" to enter "Program: CAL_READ_PR1". Open nitrogen bottle and throttle pressure to 110 psi with regulator valve. Type 0 for CRT or 1 for printer and "return".

NOTE: Both CALMODs are set in inches of mercury. CALMOD #1 should provide calibrated pressures in the range of 30, 60 and 90 percent of +/- 15 psi (30.50 in. Hg) to calibrate ZOCs #2 and #3.

- Press F2 to enter "ZOC Electronic Pressure Module Operation Menu".
- Press F4, "Read CALSYS 2000 calibration pressures". Type 2 and "return" to enter "Program: CAL_READ_PR2". Type 0 or 1 and "return".

NOTE: CALMOD #2 should provide calibrated pressures in the range of 30 ,60 and 90 percent of 50 psi (101.8 in. Hg) to calibrate ZOC #1.

- Secure nitrogen.

- Press **F2** to enter "ZOC Electronic Pressure Module Operation Menu". Press **F7**, "HP 6944A Main Menu", to enter "HP Multi-programmer (HP 6944A) Operation Menu".

3. P1 AND P2 TRANSDUCER CALIBRATION

NOTE: The procedures for the calibration of the P1 and P2 pressure transducers were modified due to the installation of a new operation/calibration solenoid valve in the instrumentation and data acquisition system.

- Press **F2**, "Calibrate Transducers (P1/P2)", to enter "Scanivalve Calibration Program". The P1 and P2 transducers are on ports 3 and 4, respectively, of the signal conditioner.
- Open the nitrogen bottle and throttle the pressure to 110 psi with the regulator valve.
- **Type 3** and "**return**", and verify channel "003" is set on the Data Acquisition/Control Unit.
- Set the solenoid valve selector handle to the "OPERATE" position.
- Zero P1 using the upper knob at port 3 on the signal conditioner.
- Set 50.9 inches of mercury on the calibration standard.
- Set the valve selector handle to the "CALIBRATE" position.
- Set +.0125 using the lower knob at port 3 on the signal conditioner.
- **Type 4** and "**return**", and verify channel "004" is set on the Data Acquisition/Control Unit.
- Repeat the above procedures for the P2 transducer.
- After both transducers are calibrated, secure the nitrogen and **Type 11** and "**return**" to enter "HP Multi-programmer (HP 6944A) Operation Menu". Press **F1**, "ZOC-14 Modules Menu" to enter "ZOC Electronic Pressure Module Operation Menu".

4. NEW_SCAN_ZOC SET-UP

- Press F1, "Scan 1-3 ZOC-14 Modules (32 ports ea)", (Program "NEW_SCAN_ZOC" will load).
- Press F3 to enter set-up parameters into the program.
- Input atmospheric pressure in psia (e.g. 14.49) and "return".
- Select data storage drive (0 is hard drive ".,700 and 1 is floppy disk drive ".,700,1") and "return".
- Input data sampling rate (330 Hz was used for current work) and "return".

NOTE: The following input scan type will determine the number of ZOC port scans. 0 and 1 allow up to 32 ports per ZOC to be scanned while 2 and 3 are automatically set at 32 ports per ZOC.

- Type 0 for single scan, 1 for multiple scans, 2 for lower blade probe survey or 3 for middle blade probe survey and "return".

*****WARNING***** If type 2 or 3 was selected, ensure the probe traverse assembly is located in the correct position for that type of survey. For a middle blade survey, it must be in the furthest downstream position that the mounting block will allow. For a lower blade survey, the mounting block may be in either the upstream or downstream position.

- Select number of samples per port (for types 0 and 1 only) and "return".
- Select number of ZOCs for recording data, (ZOC #1 is connected to the lower blade, probe and P3; ZOC #2 to the left-hand sidewall; ZOC #3 to the right-hand sidewall), and "return".
- Type 1 or 2 to enter the CALMOD number set for each ZOC.

5. DATA COLLECTION PROCEDURES

- Set nitrogen pressure to 110 psi.
- Verify position of BPV. The fully open position is suggested for the initial tunnel run of the day. Due to changing atmospheric conditions, the last position set from a previous day may not position the shocks in the design locations.

- **For scan types 2 and 3:** Verify the probe traversal lead screw and side tracks are properly lubricated and turn probe traverse motor controller on (red power light illuminates; the yellow on-line light should only illuminate when the traverse is moving).

NOTE: The next step is to **Press F4** for final preparation checklist and to begin data acquisition. The outcome will vary depending on the scan type selected.

- **For scan types 0 and 1:** **Press F4** prior to commencing tunnel operations.
- **For scan types 2 and 3:** **Press F4** at least 30 seconds prior to opening tunnel air supply valve. This will avoid placing the upward traversing probe in the unsteady initial tunnel flow. (It took the probe 42 seconds to traverse to its starting position in the current work.)

6. DATA COLLECTION

- When the tunnel pressure ratio, P2/P1, is at the desired value (displayed on the HP 9000), **Press F5** to commence data collection.
- When data collection is complete, the HP 9000 will display "Raw data completion complete" along with the raw and calibration data filenames.
- After the calibration data is collected, secure the nitrogen supply and turn off the probe motor controller.

NOTE: The raw and calibration data have been stored in files using an alphanumeric format. As an example, the data filename "ZW1312061" represents raw data (ZW), from ZOC #(1), in the year 9(3), month (12), day (6), run (1). Calibration data files begin with "ZC".

- **Press F4** to repeat the previous run using the same user input parameters as before. **Press F3** to reset "NEW_SCAN_ZOC" to step 4. **Press F6** to reduce the data or **Press F8** to exit.

7. DATA REDUCTION

- **Press F6** to reduce the current day raw data. It is recommended that all data be reduced immediately after each run to assess the results and correct the shock positioning if necessary.

NOTE: When the data reduction is complete, the reduced data file will begin with "ZR".

- **Press F8** to enter "ZOC Electronic Pressure Module Operation Menu".

8. DATA ANALYSIS

- **Press F2**, "Read reduced data from ZOC-14 module", to load the program "ZOC_MENU".

NOTE: There are two options for printing out pressure data. To list all pressures for an individual ZOC, **Type 0** and "**return**" to load the program "READ_ZOC2". This program was used by Eric Tapp in his research. To list only those pressures used in the pressure loss calculations, **Type 1** and "**return**" to load the program "NEW_READ_ZOC1". This program, initially used by Jeff Austin, plots the middle blade survey and calculates the loss coefficient data. Both programs display the "READ ZOC DATA AND DISPLAY AS SHOWN MENU".

- **For both options, Press F1**, "Input ZOC information and read data". **Input ZOC information** as prompted (i.e. 1,51218,1) and "**return**". **Type 0** or **1** and "**return**" to select data storage drive.

NOTE: Once the reduced ZOC data has been read, key **F3** will list, in columnar form, the pressures in psia for that one ZOC.

- **Press F3**, "Print pressure data to CRT or PRINTER". **Type 0** or **1** and "**return**".
- **For option 0** (program "READ_ZOC2), **Press F8**, "Exit Program" to return to "ZOC Electronic Pressure Module Operation Menu". **Press F2**, "Read reduced data from ZOC-14 module" to enter the program "ZOC_MENU". **Type 1** and "**return**" to enter the program "NEW_READ_ZOC1".
- **Press F1**, "Input ZOC information and read data". **Input ZOC information** as prompted (i.e. 1,51218,1) and "**return**". **Type 0** or **1** and "**return**" to select data storage drive. (Not required if option 1 (program NEW_READ_ZOC1) was originally used and pressures for ZOC #1 were just listed.

NOTE: Key **F5** only has meaning for ZOC #1 reduced data since it produces middle blade survey plots.

- **Press F5**, "Plot Pt Data/Print Losses". **Type 0** and "**return**" to dump plots to "Think Jet". **Press F2** to continue. After the graph appears on the CRT, **Press Shift-Dump Graph** to obtain a hard-copy. **Press F2** to continue.
- **Type 0** or **1** and "**return**" to list deviation angle and velocity data.

- **Press F2** to continue and **Type N** (No) to discontinue plotting.
- **Type 0** or **1** and **"return"** to list loss coefficient data.
- **Press F8**, "Exit Program", to enter "ZOC Electronic Pressure Module operation Menu". Return to Step 4 for additional tunnel runs.
- **Press F7**, "HP 6944A Main Menu", to return to the "HP Multi-Programmer (HP 6944A) Operation Menu".
- **Press F7**, "Main Menu", to return to the "HP 9000 Series 300 Computer Data Acquisition/Reduction System Menu".

APPENDIX B. MODIFICATIONS TO DATA ACQUISITION PROGRAMS

The original data acquisition program for the ZOC-14 Data Acquisition System was "SCAN_ZOC_05", written by Wendland [Ref. 10]. After the VELMEX NF90 stepping motor controller and UniSlide Motor Driven Assembly were made part of the wind tunnel apparatus, Myer [Ref. 7] modified the program and named it "SCAN_ZOC_06". The new program provided traversing data acquisition options for lower and middle blade surveys and continuous cascade pressure ratio displays prior to data acquisition. The filename for "SCAN_ZOC_06" in the "HP6944A" directory in the HP 9000 computer system was "NEW_SCAN_ZOC", and this was the name with which Tapp [Ref. 8] and Austin [Ref. 9] referred to the program. To prevent further confusion and ambiguity, the program was renamed "NEW_SCAN_ZOC" to match its filename.

A. CHANGES TO "NEW_SCAN_ZOC"

The "NEW_SCAN_ZOC" program had to be modified to allow for the required incrementation of the traversing probe in the cascade wake. The original data acquisition survey traverse distance behind the middle blade was 2 inches, with 33 data survey positions (32 increments) equally spaced at .0625 inches. Austin [Ref. 9] decreased the survey distance to 1.656 inches (staggered-passage width, Figure 6). The number of data survey positions remained the same (33), but the increment in distance between the middle 23 survey positions was decreased to .03125 inches to provide better spatial resolution. The increment in distance for the top 5 and bottom 5 outside survey positions was .0625 and .13125 inches, respectively.

The decision for the 33 data survey positions was based on the maximum memory size in the computer system's data collection buffer and the programming parameters for the VELMEX stepping motor controller. When all 32 ports on the 3 ZOC-14s were being used, with 10 samples being collected at each survey position, the maximum number of survey positions was 34, as shown in the following:

$$32 \times 3 \times 10 \times 34 = 32640 \text{ (Maximum Timer Counts: 32676)} \quad (\text{B.1})$$

The VELMEX was hard-wired to traverse at .0000625 inches/step, therefore, for the 2 inch survey distance with 32 increments (33 survey positions), there were a total of 32000 steps, or 1000 steps for each survey increment. The VELMEX was programmed to travel at 1000 steps/second, therefore, the parameters used in programming the 2 inch survey were fairly simplified. The 33 survey positions also allowed for an equal number of surveys above and below the blade.

The initial goal was to verify Austin's [Ref. 10] results, therefore, the same number of survey positions was used with the same increment in distance for the middle 23 positions. Instead of different outside increment in distance above and below the blade, the increments were made constant as follows:

$$[1.656 \text{ inches} - (22 \times .03125)] / 10 = .09865 \text{ inches} \quad (\text{B.2})$$

The code in "NEW_SCAN_ZOC" was modified to accommodate the the 1.656 inch middle blade survey distance, and the changes are outlined below. The parameters for programming the VELMEX are given in Reference 13.

The program was also modified to accommodate a change in the pressure ratio monitoring system. Originally, channel (pot) "0" on the signal conditioner was used for calibrating and operating the P1 100 PSID transducer, but during the present work it began to malfunction. The channel (pot) was changed to "3", and the program was modified accordingly.

1. Initialization of the Probe Start Position Above (+) the Middle Blade

Start position for 2 inch traverse: 3.312 inches above probe zero position.

$$(2 - 1.656) / 2 = .172 \text{ inches} \quad (\text{B.3})$$

$$3.312 - .172 = 3.140 \text{ inches} \quad (\text{B.4})$$

Start position for 1.656 inch traverse: 3.140 inches above probe zero position.

$$3.140 \text{ inches} / .0000625 \text{ inches/step} = +50240 \text{ steps} \quad (\text{B.5})$$

LINE 2880 OUTPUT @Traverse;"C,S1M1200,I1M50240,R"

The probe travelled 50240 steps up at 1200 steps/second. The 42 second travel time was verified with a timer.

2. Downward (-) Traverse Operation for Data Acquisition

Distance/Increment for first 5 increments: .09865 inches (From B.2)

Steps for first 5 increments:

$$.09865 \text{ inches} / .0000625 \text{ inches/step} = -1550 \text{ steps} \quad (\text{B.6})$$

**LINE 4191 IF ISCAN < 6 THEN OUTPUT @Traverse;
"C,S1M1000,I1M-1550,R"**

The probe travels 1550 steps down during each of the first 5 increments at 1000 steps/second.

Steps for next 22 increments:

$$.03125 \text{ inches} / .0000625 \text{ inches/step} = -500 \text{ steps} \quad (\text{B.7})$$

**LINE 4192 IF ISCAN < 28 THEN OUTPUT @Traverse;
"C,S1M1000,I1M-500,R"**

The probe travels 500 steps down during each of the next 22 increments at 1000 steps/second.

Steps for last 5 increments: -1550 steps (From B.6)

LINE 4200 OUTPUT @Traverse;"C,S1M1000,I1M-1550,R"

The probe travels 1550 steps down during each of the last 5 increments at 1000 steps/second.

3. Pressure Monitoring System Signal Conditioner Pot Change

LINE 3320 FOR Id = 3 TO 4 STEP 1 (Was: FOR Id = 0 TO 4 STEP 4)

LINE 3350 CASE 3 (Was: CASE 0)

B. CHANGES TO "NEW_READ_ZOC1"

Due to the changes in the survey positions, the data reduction program "NEW_READ_ZOC1" was modified. Instead of reading in each increment in distance individually, a FOR/NEXT routine was used for efficiency. To make the pressure distribution plots more readable, the parameters for the plotting subroutine were also modified.

1. Input of Blade Increment Positions

The following lines of code were added: (Y is array storing increment positions)

LINE 5135 FOR I=1 TO 33

LINE 5136 IF I<7 THEN Y(I)=(I-1)*.09685

LINE 5137 IF I>6 AND I<29 THEN Y(I)=Y(6)+(I-6)*.03125

LINE 5138 IF I>28 THEN Y(I)=Y(28)+(I-28)*.09685

LINE 5139 NEXT I

2. Parameters for Pressure Distribution Plots

Increment in distance was plotted on the "Y" axis from 1.7 to 0 in at .1 in intervals. Pressure was plotted on the "X" axis from 28 to 52 psia at 1 psia intervals. The following lines of code were changed to reflect the changes which were made:

LINE 4950 $X_0 = 28$

LINE 4960 $X_f = 52$

LINE 4970 $Y_0 = 1.7$

LINE 4980 $Y_f = 0$

LINE 4990 $D_x = 24$

LINE 5000 $D_y = 17$

APPENDIX C. PLACEMENT OF LOW-PROFILE VORTEX GENERATORS

The height (h) of the 6-5-1 low-profile, triangular plow VGs should be between $.1 \delta$ and $.5 \delta$, and the position of the VGs on the upper surfaces of the blades should be between 20δ and 30δ in front of the shock impingement [Refs. 3 and 18], which was located at $.42 C$. See Figures 2, 6, and 17-19 for the following discussion.

A. MEASUREMENT OF BOUNDARY LAYER THICKNESS

A spark shadowgraph was taken of the wind tunnel test section without any air flow. From this picture, the distance from the upper surface of the lower and middle blades was measured to the bottom of the positioning wire for each passage. The lengths of the visible portions of the lower and middle blades were also measured to compare with the lengths of the visible test section portions of the blades. A spark shadowgraph was then taken, with the camera in the same position, of the test section with the air flowing at Mach 1.4. The shock structures were positioned in the aft, start-up position on the blade, allowing a larger area forward for measuring δ . From the shadowgraph, the distance from the top of the boundary layer was measured to the bottom of the positioning wires. Table C.1 lists the measurements taken and the calculations used to determine δ follow.

	Blade Length	Shadowgraph Blade Length	Blade/Wire Clearance	δ /Wire Clearance
Middle Blade	2 3/16	2.05	0.06	0.00
Lower Blade	2 1/8	2.00	0.12	0.06

Table C.1 Boundary Layer Thickness Measurements (inches)

Therefore, the boundary layer thicknesses were determined as follows:

$$\text{Middle Blade: } \frac{2.05}{2 \frac{3}{16}} = \frac{(0.06 - 0.00)}{\delta} \quad \delta = .064 \text{ inches} \quad (\text{C.1})$$

$$\text{Lower Blade: } \frac{2.00}{2 \frac{1}{8}} = \frac{(0.12 - 0.06)}{\delta} \quad \delta = .064 \text{ inches} \quad (\text{C.2})$$

B. POSITIONING OF VORTEX GENERATORS

Leading Edge Wedge Angle = 3.5°

Blade Chord Length (C) = 6.00 inches

The shock position measured along the chord was

$$.42 \times 6.0 = 2.52 \text{ inches} \quad (\text{C.3})$$

aft of the leading edge, and the distance measured along the upper surface was,

$$2.52 / \cos(3.5^\circ) = 2.52 \text{ inches} \quad (\text{C.4})$$

aft of the leading edge. The position of the VGs in front of the shock structure should be between 20δ and 30δ , or 1.28 and 1.92 inches, respectively, giving

$$20 \times .064 = 1.28 \text{ inches} \quad (\text{C.5})$$

$$30 \times .064 = 1.92 \text{ inches} \quad (\text{C.6})$$

For ease in measuring, and to keep the VGs in front of an existing pressure port on the lower blade, the VGs were placed $1 \frac{1}{4}$ inches aft of the leading edge, which placed them 1.27 inches in front of the shock structure, approximately at the 20δ position, since

$$2.52 - 1 \frac{1}{4} = 1.27 \text{ inches} \quad (\text{C.7})$$

C. ATTACHMENT OF VORTEX GENERATORS

The VGs were attached to the upper surface of the lower and middle blades using super glue and a 5 inch diameter lighted, magnifying lens. The procedure for both blades was identical. First, using a square, light pencil lines were drawn across the blade at $1 \frac{1}{4}$ and $1 \frac{7}{16}$ inches aft of the blade leading edge, which corresponded to the positions of the leading and trailing edges of the VGs, respectively. The spacing between the VGs was 6 h, and in accordance with Figure 14, $\frac{1}{64}$ of an inch was measured and marked in from each side of the blade at the line for the VG trailing edge position. A toothpick, with glue from a glue stick, was used to pick up the VG, and the super glue was then applied to the bottom of the VG. While using the magnifying lens, the trailing edge of the first VG was aligned with its corresponding position line at the $\frac{1}{64}$ inch mark and placed on the blade surface. Another toothpick was used to adjust the position as necessary and apply pressure to the top of the VG. The excess super glue was then wiped away with a toothpick and a thin, damp cloth. The same procedure was then used to affix the VG on the opposite side of the blade. The middle 6 VGs were affixed in the same manner, but a toothpick cut to $\frac{1}{32}$ of an inch thick was used to space the VGs. Once all 8 VGs were attached to the blade, all excess super glue and the pencil lines were removed with a toothpick and the cloth.

APPENDIX D. REDUCED DATA AND NUMERICAL RESULTS

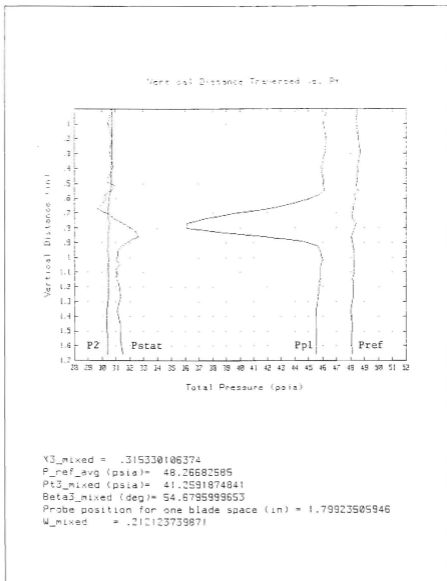
1. Aluminum Blades Without Vortex Generators

```

Data Print Out for Doc # 11, Run # 4, File#PIB10184
Period between samples (sec): 000000000000
Sample collection rate (Hz): 000
Number of samples per point: 10
Length of data run (sec): 01
The scan type is: 1
Number of scans (traverses): 00
Atmospheric pressure (psi): 14.315 psia
Tunnel Pressure Ratio (psi): 0.00147061509
    
```

Scan	Point Number						
	01	04	05	09	00	01	02
1	15.099	40.590	40.204	15.056	30.705	48.495	46.091
2	15.071	40.373	40.008	15.072	30.727	48.425	46.087
3	15.071	40.572	40.150	15.040	30.744	48.551	46.248
4	15.062	40.477	40.000	15.023	30.744	48.672	46.172
5	15.035	40.286	39.964	15.040	30.710	48.528	45.909
6	15.044	40.407	39.893	15.099	30.692	48.467	46.062
7	15.062	40.502	40.053	15.021	30.692	48.433	46.062
8	15.090	40.511	40.017	15.031	30.658	48.579	46.138
9	14.972	40.174	39.670	15.021	30.689	48.297	45.791
10	14.935	41.482	39.057	15.047	30.646	48.322	44.919
11	14.925	40.377	38.220	15.172	30.520	48.229	44.705
12	14.925	39.193	36.895	15.031	30.443	48.160	42.113
13	14.917	37.075	35.507	15.130	30.406	48.109	39.480
14	14.935	35.919	34.509	15.130	30.460	48.143	37.570
15	14.908	34.839	34.181	15.014	30.589	48.391	36.118
16	14.953	34.865	34.582	15.031	30.512	48.305	35.143
17	14.935	36.394	36.264	15.164	30.443	48.196	38.368
18	14.926	38.761	38.514	15.164	30.460	48.058	41.746
19	14.972	40.636	40.053	15.006	30.443	48.126	44.511
20	14.935	41.526	40.595	15.079	30.469	48.169	45.647
21	14.953	41.664	40.622	15.006	30.426	48.212	45.842
22	14.926	41.759	40.631	15.137	30.452	48.263	45.909
23	14.944	41.829	40.640	15.006	30.512	48.212	45.994
24	14.972	41.742	40.675	15.031	30.460	48.237	45.875
25	14.962	41.673	40.577	15.197	30.434	48.212	45.842
26	14.926	41.664	40.613	15.197	30.452	48.212	45.850
27	14.935	41.630	40.622	15.022	30.452	48.109	45.850
28	14.944	41.630	40.622	15.014	30.477	48.177	45.799
29	14.952	41.561	40.569	15.022	30.469	48.169	45.689
30	14.990	41.327	40.497	15.130	30.323	47.990	45.545
31	14.999	41.284	40.540	15.180	30.374	48.143	45.545
32	14.925	41.032	40.684	15.172	30.400	48.084	45.537
33	14.944	41.058	40.782	15.164	30.409	48.135	45.570

Input and Pressure Data: Run 1, 1/18/95



Pressure Distribution Plot and Flow Loss Results: Run 1, 1/18/95

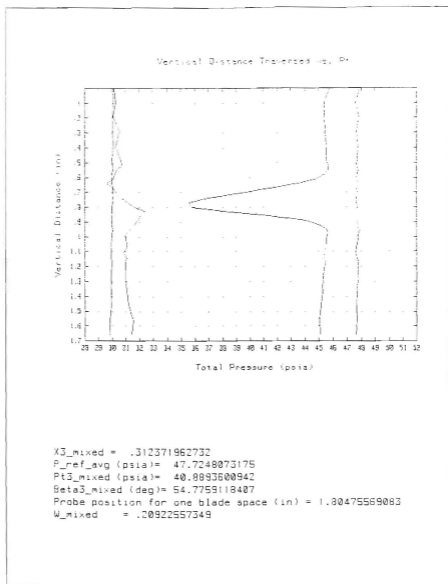
```

Data Print Out for Doc # 1 , Run # 1 , File#P15100A
Period between samples (sec) : 000000000000
Sample collection rate (Hz) : 200
Number of samples per point : 10
Length of data run (sec) : 33
The scan type is :
Number of scans/transverse : 33
Atmospheric pressure (psi) : 14.879 psia
Tunnel Pressure Ratio is : 1.39908996294

```

Scan	Port Number						
	01	04	05	06	07	08	
1	14.796	40.050	39.758	15.059	30.000	47.876	45.759
2	14.795	41.797	39.400	15.025	30.109	47.824	45.769
3	14.777	41.779	39.334	15.100	30.087	47.811	45.751
4	14.777	41.881	39.511	15.042	30.074	47.875	45.410
5	14.950	42.001	39.502	15.125	30.100	47.751	45.553
6	14.904	42.035	39.582	15.050	30.032	47.717	45.529
7	14.768	42.199	39.352	15.059	30.049	47.683	45.354
8	14.768	42.044	39.543	15.050	30.057	47.802	45.662
9	14.768	41.941	39.396	15.042	30.023	47.725	45.468
10	14.732	41.407	38.945	15.050	30.015	47.632	44.962
11	14.959	40.136	37.999	15.092	30.002	47.879	45.547
12	14.759	38.546	36.690	15.050	30.003	47.683	41.449
13	14.750	37.173	35.337	15.017	30.040	47.729	38.207
14	14.786	35.434	34.222	14.976	30.066	47.649	36.980
15	14.759	34.363	33.846	14.959	30.049	47.641	35.530
16	14.777	34.535	34.177	15.067	30.032	47.734	35.791
17	14.732	36.051	36.097	15.034	30.006	47.726	37.992
18	14.759	38.389	37.999	14.992	29.989	47.811	41.356
19	14.841	40.298	39.723	15.075	30.006	47.734	44.070
20	14.759	41.154	40.253	15.059	29.997	47.717	45.107
21	14.841	41.462	40.536	15.125	30.066	47.887	45.612
22	14.777	41.479	40.368	15.059	29.997	47.751	45.595
23	14.786	41.513	40.324	15.084	30.006	47.751	45.562
24	14.822	41.487	40.315	15.075	29.946	47.700	45.528
25	14.777	41.359	40.299	15.059	29.929	47.675	45.427
26	14.795	41.299	40.193	15.092	29.955	47.624	45.401
27	14.786	41.299	40.262	15.050	29.938	47.700	45.368
28	14.741	41.308	40.262	15.084	30.023	47.777	45.410
29	14.732	41.171	40.253	15.075	29.963	47.794	45.309
30	14.723	41.000	40.386	15.100	29.929	47.709	45.250
31	14.714	40.948	40.368	15.050	29.929	47.649	45.174
32	14.660	40.777	40.474	15.000	29.961	47.726	45.022
33	14.732	40.726	40.588	15.025	29.843	47.581	45.107

Input and Pressure Data: Run 2, 1/24/95

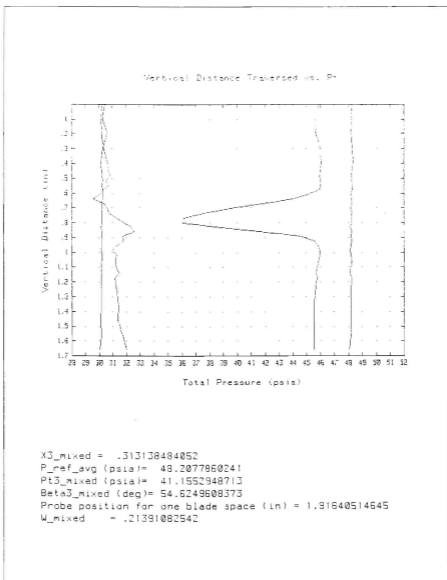


Pressure Distribution Plot and Flow Loss Results: Run 2, 1/24/95

Data Point Out For Iso # 1, Run # 1, File#R1910240
 Period between samples (sec): 00300303000
 Sample collection rate (Hz): 100
 Number of samples per port: 10
 Length of data run (sec): 31
 The span type is: 0
 Number of scans/inverses: 30
 Atmospheric pressure is: 14.585 psia
 Tunnel Pressure Ratio is: 1.880541589

Scan	Port Number						
	01	04	05	09	10	31	32
1	14.963	42.198	39.398	15.257	30.226	48.216	45.899
2	14.954	42.017	39.589	15.217	30.184	48.207	45.822
3	14.972	42.120	39.542	15.242	30.211	48.198	45.839
4	14.972	42.292	39.319	15.275	30.288	48.258	45.941
5	14.936	42.404	39.387	15.250	30.175	48.251	45.851
6	14.963	42.386	39.342	15.250	30.229	48.241	45.967
7	14.990	42.412	39.989	15.242	30.205	48.258	46.017
8	14.999	42.404	39.369	15.250	30.253	48.309	46.017
9	14.963	42.501	39.774	15.250	30.286	48.256	45.925
10	14.990	41.874	39.041	15.242	30.288	48.190	45.100
11	15.026	40.773	38.085	15.256	30.288	48.232	44.016
12	15.017	39.004	36.971	15.242	30.262	48.258	44.794
13	15.008	37.312	35.662	15.225	30.236	48.198	39.584
14	14.963	35.903	34.538	15.242	30.236	48.258	37.542
15	15.026	34.897	34.034	15.257	30.229	48.258	36.143
16	14.972	34.785	34.396	15.258	30.229	48.224	36.042
17	14.954	36.487	36.079	15.209	30.202	48.096	36.342
18	14.972	38.543	38.342	15.242	30.229	48.241	41.550
19	14.981	40.713	39.372	15.233	30.211	48.156	44.503
20	14.990	41.502	40.605	15.233	30.219	48.224	45.529
21	14.999	41.591	40.659	15.233	30.211	48.173	45.324
22	14.972	41.751	40.614	15.233	30.176	48.199	45.941
23	14.927	41.863	40.650	15.217	30.229	48.156	45.941
24	14.981	41.829	40.588	15.275	30.262	48.232	45.899
25	15.008	41.760	40.570	15.233	30.194	48.249	45.940
26	14.945	41.674	40.552	15.225	30.159	48.113	45.748
27	14.981	41.700	40.597	15.242	30.202	48.096	45.740
28	14.981	41.648	40.526	15.217	30.202	48.258	45.765
29	14.954	41.485	40.552	15.225	30.159	48.190	45.613
30	15.017	41.399	40.579	15.225	30.151	48.164	45.546
31	14.900	41.271	40.594	15.209	30.125	48.173	45.546
32	14.945	41.193	40.379	15.225	30.151	48.181	45.521
33	14.981	41.176	41.030	15.217	30.091	48.088	45.521

Input and Pressure Data: Run 3, 1/24/95



Pressure Distribution Plot and Flow Loss Results: Run 3, 1/24/95

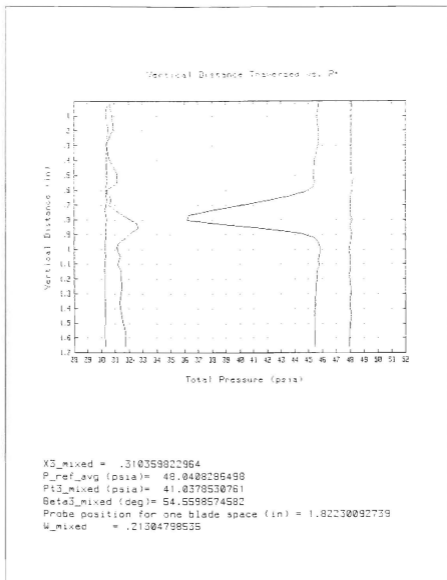
```

Data Print Out For Job # 1 , Run # 3 , File#R1510043
Period between samples (sec) : 00.0000000000
Sample collection rate (Hz) : 000
Number of samples per point : 10
Length of data run (sec) : 37
The scan type is : 0
Number of scans/traverses : 33
Atmospheric pressure is : 14.878 psia
Tunnel Pressure Ratio is : 2.00970016293

```

Scan	Port Number						
	01	04	05	08	09	11	22
1	14.928	42.160	39.314	15.159	30.468	48.116	45.796
2	14.919	42.051	39.725	15.134	30.423	48.049	45.600
3	14.910	42.005	39.779	15.225	30.500	48.065	45.719
4	14.901	42.103	39.725	15.134	30.406	48.065	45.744
5	14.919	41.954	39.567	15.201	30.431	48.090	45.415
6	14.883	41.957	39.627	15.175	30.388	48.090	45.381
7	14.901	41.948	39.646	15.175	30.388	48.219	45.381
8	14.919	42.068	39.637	15.167	30.423	48.167	45.449
9	14.883	41.965	39.363	15.159	30.271	48.099	45.297
10	14.874	41.382	39.896	15.175	30.380	48.107	44.749
11	14.865	40.388	38.140	15.134	30.337	47.989	43.475
12	14.883	39.995	37.802	15.151	30.380	48.031	41.771
13	14.919	37.840	35.799	15.167	30.354	48.031	39.861
14	14.946	36.278	34.952	15.134	30.303	47.989	37.914
15	14.946	35.068	34.224	15.175	30.260	48.031	36.293
16	14.946	35.025	34.542	15.159	30.414	48.150	36.183
17	14.883	36.373	36.197	15.142	30.346	47.980	38.235
18	14.901	38.801	38.267	15.159	30.329	47.997	41.595
19	14.946	40.611	40.009	15.192	30.346	48.141	44.394
20	14.874	41.434	40.557	15.142	30.329	48.039	45.457
21	14.883	41.614	40.592	15.167	30.294	47.980	45.744
22	14.892	41.700	40.574	15.167	30.312	47.963	45.820
23	14.901	41.700	40.574	15.192	30.312	47.937	45.811
24	14.901	41.700	40.557	15.184	30.346	48.022	45.752
25	14.910	41.614	40.539	15.167	30.294	47.980	45.710
26	14.882	41.674	40.521	15.251	30.296	48.014	45.752
27	14.847	41.537	40.495	15.142	30.260	47.997	45.584
28	14.874	41.537	40.548	15.175	30.277	47.929	45.689
29	14.901	41.460	40.574	15.175	30.277	48.048	45.587
30	14.910	41.314	40.521	15.167	30.277	48.022	45.491
31	14.928	41.271	40.583	15.159	30.296	48.073	45.440
32	14.892	41.288	40.680	15.142	30.260	47.963	45.457
33	14.919	41.211	40.725	15.167	30.277	47.971	45.432

Input and Pressure Data: Run 4, 1/24/95



Pressure Distribution Plot and Flow Loss Results: Run 4, 1/24/95

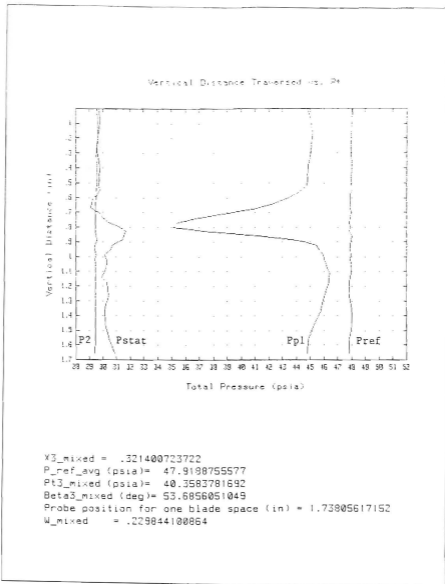
2. Aluminum Blades With Vortex Generators

```

Data Print Out for Job # 1, Run # 1, File#P151451
Period between samples: sec = 0.001000000000
Sample collection rate: Hz = 1000
Number of samples per point = 10
Length of data run: sec = 33
The scan type is: 3
Number of scans/traverses: 33
Atmospheric pressure (psi) = 14.891 data
Tunnel Pressure Ratio (psi) = 1.96292171816
    
```

Scan	Point Number						
	01	04	05	09	10	31	32
1	14.840	41.184	38.843	15.857	29.551	48.833	44.305
2	14.795	41.468	39.137	15.816	29.582	47.888	45.186
3	14.795	41.526	39.079	15.822	29.585	47.929	45.150
4	14.831	41.355	39.035	14.982	29.491	47.845	45.017
5	14.795	41.321	38.917	15.832	29.534	48.022	44.867
6	14.795	41.312	38.916	15.849	29.534	47.937	44.805
7	14.831	41.235	38.757	15.849	29.550	47.929	44.725
8	14.822	41.029	38.445	15.840	29.491	47.988	44.363
9	14.804	40.852	38.117	14.999	29.534	47.983	43.929
10	14.804	40.801	37.468	15.907	29.474	47.869	43.186
11	14.795	39.316	36.983	14.966	29.423	47.912	42.362
12	14.786	38.331	35.925	15.840	29.440	47.886	41.853
13	14.804	36.918	34.863	14.982	29.415	47.920	39.866
14	14.804	35.368	33.751	15.832	29.449	47.886	38.963
15	14.741	34.246	33.127	15.849	29.449	47.861	38.408
16	14.804	34.084	33.448	14.982	29.405	47.983	35.891
17	14.786	35.888	35.824	15.840	29.440	47.844	37.272
18	14.831	38.288	37.510	15.824	29.517	47.980	41.178
19	14.867	40.453	39.314	15.840	29.551	47.954	44.071
20	14.795	41.398	40.140	15.865	29.398	47.886	45.460
21	14.804	41.621	40.216	14.966	29.363	47.869	45.690
22	14.822	41.749	40.249	15.849	29.466	47.937	45.929
23	14.804	41.825	40.393	14.982	29.398	47.869	46.027
24	14.822	41.946	40.435	15.816	29.457	47.920	46.133
25	14.831	41.998	40.536	15.849	29.423	47.929	46.257
26	14.768	42.066	40.612	15.824	29.440	47.929	46.389
27	14.768	42.066	40.582	15.832	29.432	47.878	46.363
28	14.840	42.066	40.645	15.824	29.432	47.861	46.363
29	14.777	41.792	40.418	15.824	29.406	47.852	46.000
30	14.822	41.492	40.266	15.857	29.440	48.014	45.773
31	14.822	41.047	39.971	15.840	29.423	47.988	45.255
32	14.813	40.712	39.786	15.849	29.449	47.852	44.840
33	14.849	40.695	39.912	15.824	29.355	47.852	44.796

Input and Pressure Data: Run 1, 2/15/95

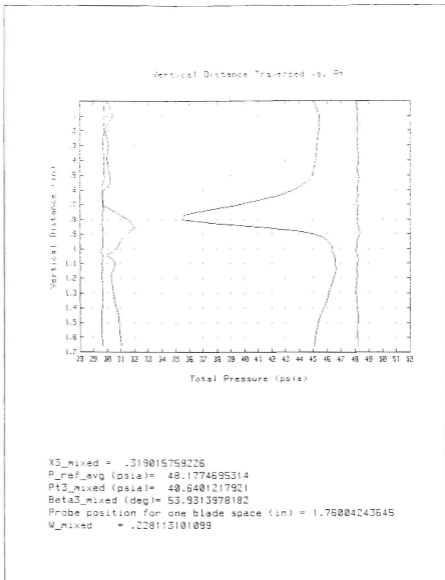


Pressure Distribution Plot and Flow Loss Results: Run 1, 2/15/95

Data Print Out for Doc # 1 , Run # 2 , File#R151492
 Period between samples : sec : 000000000003
 Sample collection rate : Mode : 000
 Number of samples per point : 10
 Length of data run : sec : 31
 The scan type is : 0
 Number of scans/traverses : 33
 Atmospheric pressure is : 14.8228 psia
 Tunnel Pressure Ratio is : 1.37106793148

Scan	01	04	05	09	20	31	32
1	14.952	41.140	39.149	15.105	29.773	48.124	45.930
2	14.997	41.345	39.911	15.197	29.791	48.157	45.411
3	14.952	41.742	39.402	15.063	29.756	48.175	45.437
4	14.888	41.639	39.369	15.114	29.714	48.158	45.279
5	14.970	41.622	39.191	15.105	29.756	48.219	45.190
6	14.961	41.493	39.002	15.130	29.755	48.175	44.968
7	14.988	41.511	39.031	15.155	29.815	48.203	44.533
8	14.933	41.262	38.694	15.147	29.714	48.209	44.543
9	14.979	40.934	38.332	15.155	29.611	48.192	44.048
10	14.924	40.328	37.692	15.072	29.679	48.192	43.420
11	14.924	39.549	37.094	15.105	29.748	48.235	42.528
12	14.933	39.426	36.849	15.130	29.662	48.107	40.986
13	14.970	37.140	35.071	15.122	29.739	48.209	39.402
14	14.943	35.751	34.127	15.147	29.696	48.201	37.322
15	14.979	34.500	33.453	15.139	29.671	48.192	35.567
16	14.906	34.422	33.773	15.097	29.637	48.158	35.436
17	14.879	35.992	35.223	15.122	29.629	48.175	37.623
18	14.970	38.734	38.012	15.147	29.679	48.252	41.658
19	14.915	40.351	39.764	15.164	29.722	48.320	44.805
20	14.997	41.742	40.320	15.164	29.645	48.209	45.694
21	14.933	41.990	40.589	15.114	29.689	48.098	45.092
22	14.970	42.204	40.673	15.230	29.637	48.132	46.331
23	14.979	42.093	40.623	15.089	29.560	48.056	46.331
24	14.961	42.144	40.673	15.147	29.645	48.150	46.525
25	14.924	42.247	40.950	15.172	29.654	48.218	46.552
26	14.915	42.239	40.892	15.097	29.629	48.158	46.552
27	14.943	42.272	40.917	15.114	29.654	48.107	46.323
29	14.933	42.179	40.850	15.122	29.611	48.158	46.570
29	14.906	41.887	40.715	15.130	29.637	48.039	46.251
30	14.979	41.648	40.555	15.222	29.645	48.115	45.941
31	14.924	41.279	40.353	15.155	29.628	48.226	45.481
32	14.943	40.954	40.261	15.164	29.628	48.192	45.189
33	14.924	40.902	40.235	15.130	29.645	48.235	45.110

Input and Pressure Data: Run 2, 2/15/95

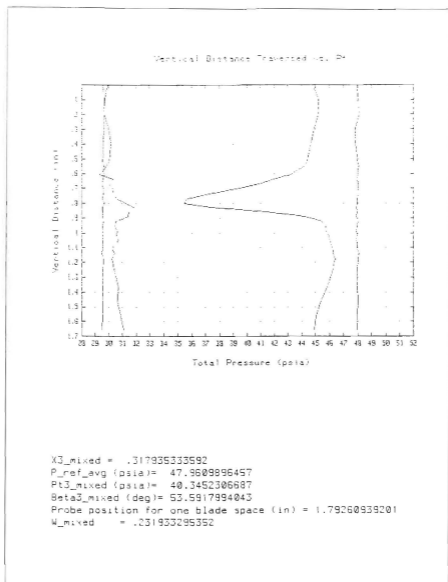


Pressure Distribution Plot and Flow Loss Results: Run 2, 2/15/95

Data Print Out for Job # 1, Run # 3, File # CR1514183
 Period between samples used: 003030303030
 Sample collection rate: Mode: 000
 Number of samples per point: 10
 Length of data run / sec: 31
 The scan type is: 1
 Number of scans/traversals: 33
 Atmospheric pressure is: 14.884 psia
 Tunnel Pressure Ratio is: 1.9534310841

Scan	Port Number						
	01	04	05	08	09	31	32
1	14.957	41.295	38.975	15.087	29.525	47.957	44.920
2	14.992	41.335	39.152	15.104	29.569	48.001	45.135
3	14.957	41.579	39.129	15.112	29.542	48.095	45.203
4	14.957	41.330	39.077	15.079	29.568	47.930	44.937
5	14.929	41.320	38.940	15.120	29.588	47.956	44.706
6	14.948	41.088	38.720	15.112	29.525	47.941	44.485
7	14.948	41.114	38.552	15.112	29.565	47.975	44.405
8	14.866	40.933	38.292	15.171	29.560	48.044	44.245
9	14.957	40.529	37.944	15.184	29.517	47.992	43.730
10	14.920	39.954	37.571	15.079	29.560	48.018	43.198
11	14.920	39.326	36.978	15.112	29.583	47.924	41.965
12	14.957	38.373	36.082	15.157	29.506	48.019	40.974
13	14.975	37.196	35.075	15.137	29.526	47.984	39.134
14	14.975	35.718	34.110	15.146	29.500	48.052	37.299
15	14.930	34.463	32.365	15.095	29.568	47.933	35.864
16	14.902	34.325	33.586	15.112	29.643	47.967	35.425
17	14.957	35.838	35.101	15.095	29.557	47.907	37.386
18	14.930	38.459	37.563	15.154	29.523	47.941	41.362
19	14.866	40.512	39.508	15.146	29.574	47.873	44.219
20	14.902	41.432	39.973	15.162	29.508	48.009	45.434
21	14.812	41.655	40.193	15.087	29.566	47.941	45.735
22	14.911	41.775	40.236	15.112	29.531	47.873	45.797
23	14.957	41.930	40.295	15.129	29.548	47.924	45.948
24	14.975	41.930	40.147	15.137	29.574	47.898	46.028
25	14.984	42.007	40.489	15.137	29.548	47.924	46.143
26	14.948	42.053	40.422	15.112	29.557	47.924	46.214
27	14.984	42.050	40.574	15.162	29.497	48.061	46.250
28	14.933	42.127	40.608	15.146	29.565	48.001	46.383
29	14.866	41.999	40.532	15.120	29.557	47.958	46.188
30	14.929	41.698	40.422	15.154	29.523	47.933	45.959
31	14.884	41.225	40.126	15.171	29.531	48.001	45.354
32	14.866	40.985	39.999	15.146	29.548	47.975	45.043
33	14.884	40.744	40.143	15.137	29.497	47.975	44.910

Input and Pressure Data: Run 3, 2/15/95

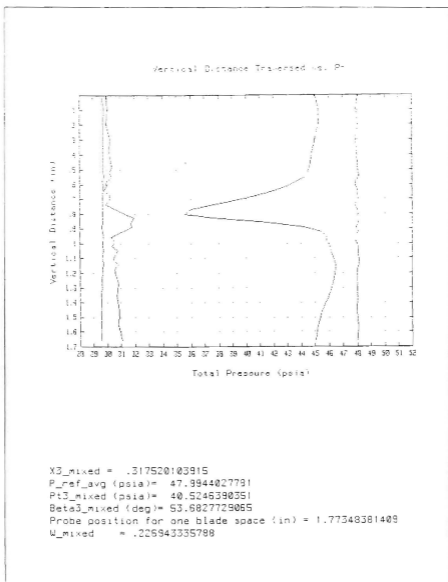


Pressure Distribution Plot and Flow Loss Results: Run 3, 2/15/95

Data Print Out for Job # 1 , Run # 4 , File#R151415#
 Period between samples (sec) : .0010103030300
 Sample collection rate (Hz) : 100
 Number of samples per point : 10
 Length of data run (sec) : 31
 The scan type is : 3
 Number of scans/traverses : 30
 Atmospheric pressure is : 14.591 psi
 Tunnel Pressure Ratio is : 1.97576759853

Scan	01	Port Number 24	25	26	30	31	32
1	14.909	41.352	39.175	14.998	29.532	48.047	45.011
2	14.908	41.587	39.277	15.092	29.761	47.894	45.257
3	14.959	41.518	39.327	15.040	29.737	48.081	45.295
4	14.844	41.515	39.150	15.099	29.744	47.863	45.020
5	14.862	41.360	38.997	15.073	29.735	47.871	44.334
6	14.990	41.293	38.848	15.055	29.744	47.995	44.821
7	14.962	41.163	38.718	15.056	29.592	48.090	44.515
8	14.935	41.120	38.481	15.056	29.761	48.107	44.279
9	14.908	40.685	38.867	15.115	29.684	47.977	43.763
10	14.935	40.029	37.593	15.092	29.592	47.983	43.073
11	14.899	39.333	36.924	15.090	29.701	47.988	42.197
12	14.899	38.474	36.137	15.056	29.667	47.998	40.913
13	14.872	37.289	35.206	15.065	29.658	48.073	39.390
14	14.853	35.742	34.182	15.107	29.684	47.809	37.592
15	14.853	34.668	33.590	15.048	29.675	48.022	36.006
16	14.899	34.504	33.840	15.040	29.684	48.039	35.546
17	14.926	35.008	35.206	15.082	29.549	47.928	37.530
18	14.917	38.595	37.796	15.090	29.684	48.039	41.553
19	14.853	40.648	39.547	15.073	29.832	47.954	44.223
20	14.908	41.541	40.131	15.065	29.558	48.047	45.453
21	14.899	41.679	40.224	15.115	29.701	47.851	45.816
22	14.917	41.941	40.287	15.073	29.841	47.983	45.860
23	14.925	41.962	40.368	15.115	29.675	48.056	46.090
24	14.908	42.013	40.529	15.090	29.718	48.039	46.125
25	14.925	42.062	40.589	15.082	29.658	48.047	46.249
26	14.908	42.219	40.580	15.107	29.667	48.132	46.373
27	14.881	42.229	40.817	15.115	29.692	48.107	46.435
28	14.925	42.219	40.741	15.073	29.658	47.988	46.461
29	14.917	42.150	40.732	15.056	29.624	47.979	46.320
30	14.881	41.798	40.512	15.107	29.555	48.005	45.975
31	14.926	41.369	40.389	15.115	29.538	47.954	45.515
32	14.853	40.991	40.192	15.107	29.564	48.047	45.196
33	14.881	40.769	40.258	15.058	29.555	47.979	45.011

Input and Pressure Data: Run 4, 2/15/95



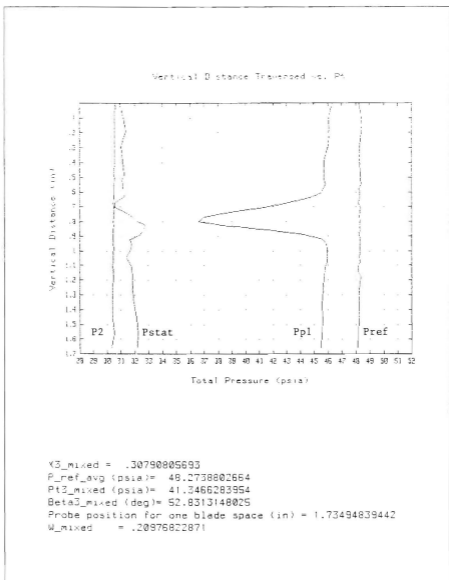
Pressure Distribution Plot and Flow Loss Results: Run 4, 2/15/95

3. Steel Blades Without Vortex Generators

Data Print Out for Job # 1, Run # 1, Rate R1S14241
 Period between samples used: 0.001000000000
 Sample collection rate used: 000
 Number of samples per point: 10
 Length of data run used: 01
 The scan type is: 0
 Number of spans (inverses): 00
 Atmospheric pressure is: 14.7925 psia
 Tunnel Pressure Ratio is: 0.005000000000

Scan	Q1	Point Number					
		24	25	26	30	31	32
1	14.819	40.649	40.268	39.276	30.459	48.216	46.314
2	14.792	40.638	40.116	39.334	30.386	48.285	46.257
3	14.827	40.672	40.108	39.294	30.586	48.294	46.289
4	14.809	40.495	39.997	39.251	30.395	48.217	46.204
5	14.773	40.290	39.862	39.293	30.586	48.300	45.747
6	14.900	42.323	39.320	39.259	30.543	48.260	45.712
7	14.773	42.314	39.303	39.294	30.652	48.377	45.747
8	14.819	42.363	39.370	39.294	30.543	48.395	45.909
9	14.927	42.331	39.735	39.234	30.509	48.232	45.885
10	14.927	42.323	39.600	39.259	30.519	48.291	45.517
11	14.746	41.747	38.963	39.268	30.525	48.200	44.720
12	14.836	40.303	37.754	39.226	30.475	48.199	43.170
13	14.819	38.971	36.482	39.276	30.519	48.334	41.362
14	14.782	37.235	35.291	39.209	30.535	48.256	38.835
15	14.764	35.945	34.501	39.234	30.501	48.215	37.819
16	14.854	35.584	34.527	39.268	30.483	48.308	36.584
17	14.818	36.882	35.882	39.219	30.501	48.283	38.297
18	14.900	39.866	37.340	39.259	30.466	48.309	41.548
19	14.782	41.808	39.616	39.226	30.475	48.240	44.295
20	14.819	41.867	40.311	39.226	30.449	48.266	45.505
21	14.773	42.142	40.472	39.234	30.458	48.291	45.871
22	14.900	42.263	40.446	39.259	30.492	48.300	45.951
23	14.764	42.185	40.429	39.192	30.466	48.274	45.933
24	14.782	42.151	40.370	39.259	30.441	48.223	45.924
25	14.764	42.160	40.463	39.276	30.466	48.274	45.924
26	14.809	42.108	40.395	39.243	30.432	48.164	45.900
27	14.791	42.065	40.421	39.268	30.458	48.172	45.791
28	14.782	42.013	40.429	39.276	30.466	48.326	45.738
29	14.791	41.910	40.404	39.192	30.381	48.223	45.658
30	14.764	41.807	40.438	39.259	30.389	48.249	45.570
31	14.900	41.764	40.565	39.219	30.406	48.249	45.579
32	14.792	41.721	40.658	39.268	30.492	48.181	45.561
33	14.782	41.575	40.666	39.251	30.355	48.138	45.499

Input and Pressure Data: Run 1, 2/24/95

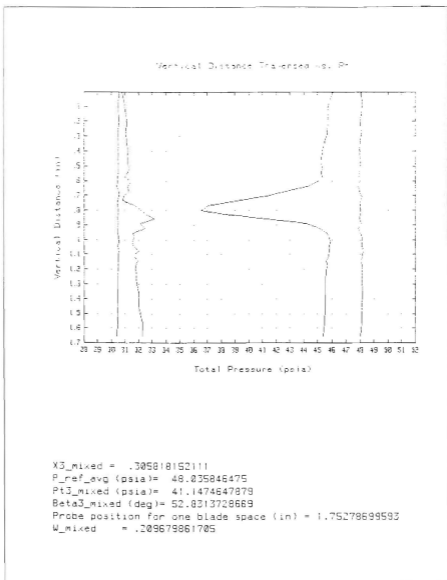


Pressure Distribution Plot and Flow Loss Results: Run 1, 2/24/95

Data Print Out for Job # 1, Run # 2, File#P1514140
 Period between samples sec : 0.000000000000
 Sample collection rate Hz : 20
 Number of samples per point : 10
 Length of data run sec : 31
 The scan type is: 0
 Number of scans/transverse: 20
 Atmospheric pressure is: 14.7912 psia
 Tunnel Pressure Ratio is: 0.01914010957

Scan	Point Number						
	01	24	25	28	30	31	32
1	14.799	40.415	40.053	15.140	30.573	48.073	45.053
2	14.762	40.214	39.821	15.175	30.544	48.116	45.720
3	14.771	40.275	39.891	15.159	30.570	48.021	45.747
4	14.771	40.163	39.350	15.159	30.535	48.064	45.958
5	14.771	41.964	39.584	15.175	30.544	47.936	45.320
6	14.790	41.982	39.491	15.193	30.527	48.021	45.277
7	14.744	40.033	39.553	15.175	30.527	47.996	45.312
8	14.799	41.990	39.483	15.159	30.501	47.961	45.285
9	14.771	41.999	39.423	15.159	30.484	47.884	45.294
10	14.771	41.995	39.279	15.169	30.484	47.827	45.001
11	14.790	41.525	38.602	15.151	30.424	47.816	44.238
12	14.726	40.171	37.594	15.151	30.552	47.944	42.711
13	14.771	39.998	36.510	15.159	30.552	48.098	41.236
14	14.755	37.021	35.274	15.175	30.484	48.030	39.842
15	14.771	35.925	34.477	15.159	30.458	47.996	37.034
16	14.762	35.573	34.486	15.168	30.492	47.987	36.545
17	14.753	36.789	35.756	15.175	30.492	47.996	38.242
18	14.762	39.084	37.865	15.151	30.441	47.953	41.254
19	14.762	40.378	39.406	15.175	30.501	48.073	44.158
20	14.798	41.792	40.016	15.113	30.466	47.950	45.099
21	14.744	42.016	40.253	15.184	30.449	48.013	45.685
22	14.916	42.180	40.355	15.258	30.544	48.107	45.853
23	14.762	42.197	40.304	15.226	30.570	48.124	45.971
24	14.807	42.120	40.380	15.210	30.484	48.133	45.927
25	14.762	42.171	40.473	15.218	30.552	48.236	45.827
26	14.753	42.042	40.346	15.260	30.509	48.193	45.774
27	14.762	41.964	40.346	15.201	30.509	47.996	45.605
28	14.790	41.990	40.355	15.201	30.518	48.116	45.685
29	14.780	41.887	40.287	15.210	30.475	48.124	45.561
30	14.789	41.792	40.439	15.193	30.458	48.150	45.543
31	14.755	41.654	40.558	15.201	30.458	48.116	45.525
32	14.799	41.563	40.651	15.235	30.458	48.141	45.498
33	14.771	41.507	40.660	15.201	30.398	47.996	45.401

Input and Pressure Data: Run 2, 2/24/95



Pressure Distribution Plot and Flow Loss Results: Run 2, 2/24/95

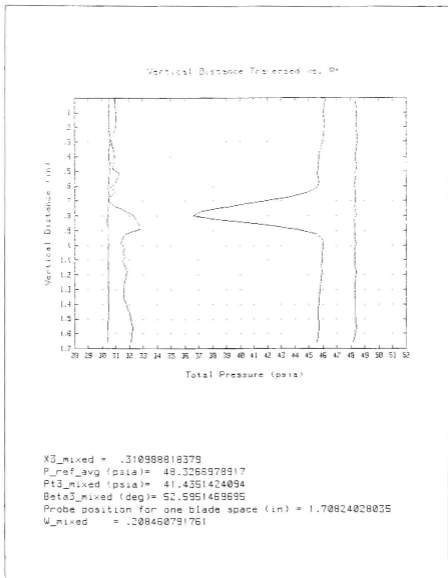
```

Data Print Out for Test # 1, Run # 1, File#R1514244
Period between samples used : 0.001000000000
Sample collection rate: 100
Number of samples per point: 10
Length of data run used: 33
The span type is: 3
Number of scans/inverses: 33
Atmospheric pressure is: 14.7723 psia
Tunnel Pressure Ratio is: 2.0014479152

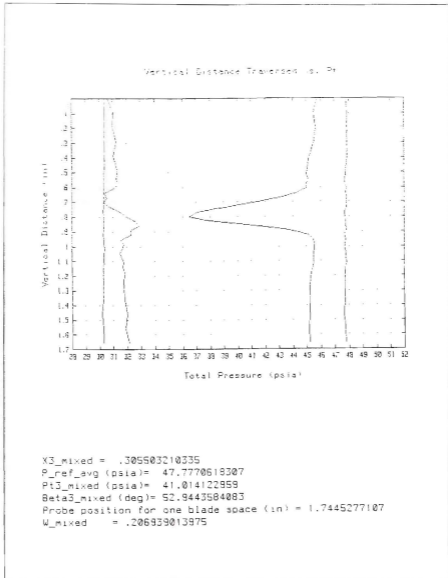
```

Scan	Point Number						
	01	14	25	28	30	31	32
1	14.755	40.554	40.172	15.257	30.536	48.325	46.197
2	14.792	40.477	40.079	15.291	30.529	48.394	46.055
3	14.774	40.554	40.110	15.274	30.529	48.420	46.108
4	14.774	40.407	39.977	15.299	30.596	48.454	46.029
5	14.746	40.225	39.918	15.255	30.510	48.377	45.744
6	14.801	40.140	39.706	15.307	30.579	48.429	45.646
7	14.774	40.235	39.755	15.307	30.553	48.274	45.502
8	14.754	40.255	39.755	15.257	30.545	48.334	45.591
9	14.754	40.356	39.740	15.274	30.502	48.283	45.735
10	14.755	40.243	39.477	15.215	30.442	48.265	45.602
11	14.754	41.898	39.027	15.291	30.519	48.343	44.853
12	14.774	40.919	38.051	15.299	30.536	48.343	43.727
13	14.792	39.101	36.583	15.274	30.502	48.343	41.557
14	14.755	37.470	35.446	15.224	30.450	48.291	39.334
15	14.910	36.071	34.540	15.224	30.442	48.325	37.270
16	14.801	35.680	34.522	15.232	30.450	48.428	36.559
17	14.737	36.074	35.794	15.224	30.415	48.257	38.365
18	14.719	39.162	37.999	15.215	30.424	48.274	41.558
19	14.810	41.025	39.451	15.232	30.459	48.274	44.055
20	14.746	41.933	40.215	15.249	30.467	48.283	45.566
21	14.746	42.192	40.402	15.249	30.450	48.300	45.948
22	14.737	42.295	40.334	15.299	30.510	48.385	46.002
23	14.728	42.338	40.452	15.282	30.485	48.291	46.029
24	14.746	42.252	40.402	15.274	30.459	48.300	45.957
25	14.801	42.261	40.419	15.274	30.459	48.255	45.948
26	14.746	42.251	40.402	15.282	30.485	48.300	45.366
27	14.737	42.200	40.393	15.299	30.467	48.300	45.895
28	14.774	42.218	40.503	15.274	30.485	48.429	45.330
29	14.754	42.062	40.419	15.255	30.467	48.300	45.833
30	14.728	41.907	40.410	15.257	30.459	48.308	45.726
31	14.783	41.907	40.495	15.282	30.459	48.291	45.654
32	14.754	41.907	40.673	15.292	30.424	48.385	45.708
33	14.719	41.796	40.622	15.299	30.433	48.205	45.628

Input and Pressure Data: Run 3, 2/24/95



Pressure Distribution Plot and Flow Loss Results: Run 3, 2/24/95



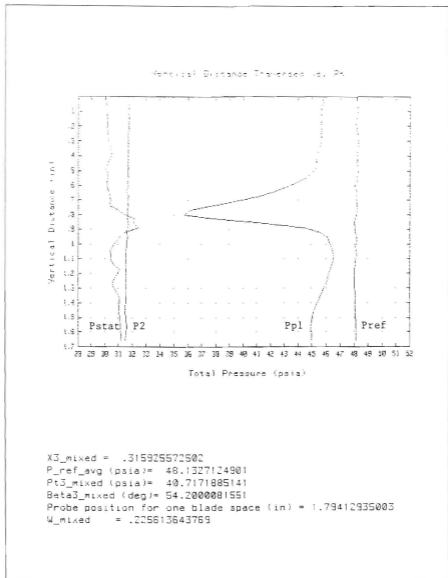
Pressure Distribution Plot and Flow Loss Results: Run 4, 2/24/95

4. Steel Blades With Vortex Generators

Data Prints Out for Case 4.1, Run # 10, File# 01501410
 Period between samples: sec: 1.0000000000000000
 Sample collection rate: Hz: 100
 Number of samples per point: 10
 Length of data run used: 31
 The scan type is: 3
 Number of scans/traverses: 33
 Atmospheric pressure is: 14.7894 psia
 Tunnel Pressure Ratio is: 2.07879055556

Scan	Port Number						
	01	04	05	08	30	32	
1	14.752	42.050	39.794	15.254	31.731	48.189	45.858
2	14.907	41.987	39.726	15.291	31.755	48.222	45.863
3	14.790	41.940	39.701	15.254	31.755	48.147	45.872
4	14.752	41.940	39.743	15.281	31.714	48.274	45.872
5	14.816	41.820	39.541	15.205	31.722	48.232	45.939
6	14.916	41.823	39.505	15.289	31.714	48.240	45.240
7	14.843	41.554	39.857	15.279	31.731	48.274	44.894
8	14.753	41.563	38.741	15.314	31.714	48.138	44.586
9	14.852	40.801	38.296	15.256	31.637	48.257	43.377
10	14.744	40.185	37.758	15.272	31.748	48.011	43.218
11	14.744	35.812	37.889	15.347	31.534	48.198	42.344
12	14.907	38.827	36.542	15.247	31.755	48.13	41.240
13	14.771	37.532	35.489	15.314	31.637	48.189	39.633
14	14.825	36.935	34.511	15.231	31.714	48.189	37.932
15	14.834	34.949	32.795	15.272	31.679	48.181	36.154
16	14.825	34.632	33.887	15.272	31.679	48.121	35.712
17	14.753	36.199	35.531	15.305	31.671	48.052	37.786
18	14.725	38.679	38.075	15.297	31.731	48.002	41.620
19	14.861	40.758	40.131	15.198	31.671	48.087	44.445
20	4.762	41.632	40.478	15.272	31.619	48.079	45.628
21	14.807	41.897	40.745	15.247	31.654	48.181	46.095
22	14.807	41.991	40.745	15.231	31.611	48.198	46.237
23	14.798	41.955	40.821	15.214	31.611	48.053	46.334
24	14.887	42.137	40.762	15.264	31.551	48.104	46.440
25	14.816	42.137	40.863	15.254	31.551	48.155	46.493
26	14.834	42.179	40.804	15.272	31.560	48.053	46.493
27	14.744	42.154	40.529	15.281	31.577	48.087	45.431
28	14.789	42.129	40.821	15.289	31.543	48.028	46.290
29	14.780	41.709	40.568	15.239	31.543	48.002	45.999
30	14.798	41.583	40.316	15.281	31.551	48.070	45.540
31	14.771	41.007	40.000	15.231	31.508	48.036	45.053
32	14.834	40.810	40.072	15.148	31.502	48.104	44.895
33	14.843	40.784	40.274	15.247	31.500	48.096	44.993

Input and Pressure Data: Run 1, 3/14/95

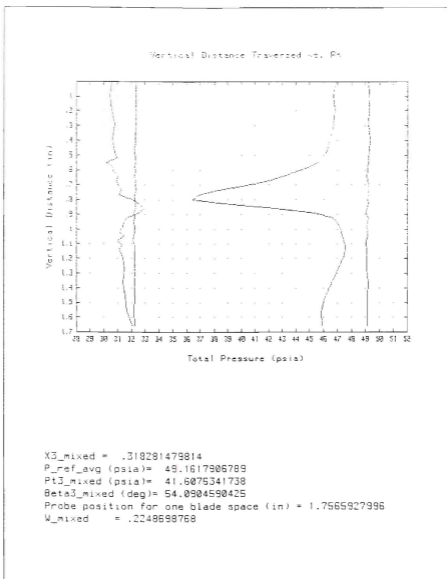


Pressure Distribution Plot and Flow Loss Results: Run 1, 3/14/95

Data Print Out for Doc # 1 , Run # 11 , File#R15001401
 Period between samples (sec): 0.003000000000
 Sample collection rate (Hz): 330
 Number of samples per point: 10
 Length of data run (sec): 33
 The scan type is: 7
 Number of spans/traverses: 33
 Atmospheric pressure is: 14.3042 psia
 Tunnel Pressure Ratio is: 0.06356648795

Scan	01	Port Number 04	05	06	30	01	02
1	14.752	42.991	40.579	15.821	32.358	49.230	46.944
2	14.751	42.319	40.582	15.690	32.333	49.247	46.792
3	14.776	42.996	40.645	15.614	32.341	49.256	46.819
4	14.795	42.379	40.662	15.656	32.341	49.198	46.635
5	14.795	42.750	40.293	15.631	32.291	49.307	46.472
6	14.748	42.570	40.080	15.631	32.278	49.273	46.172
7	14.731	42.381	39.878	15.481	32.215	49.199	45.371
8	14.694	41.969	39.632	15.631	32.264	49.205	45.687
9	14.658	41.609	39.220	15.548	32.230	49.129	45.012
10	14.787	40.982	38.461	15.656	32.291	49.171	44.865
11	14.731	40.252	37.922	15.515	32.256	49.066	43.891
12	14.740	39.403	37.196	15.406	32.281	49.171	42.828
13	14.667	38.236	36.178	15.606	32.290	49.213	40.372
14	14.795	36.656	35.130	15.656	32.333	49.230	38.308
15	14.803	35.446	34.304	15.606	32.230	49.205	36.846
16	14.740	35.309	34.498	15.548	32.221	49.129	36.394
17	14.722	36.890	36.260	15.656	32.273	49.213	38.680
18	14.731	39.557	38.874	15.681	32.264	49.111	42.471
19	14.749	41.634	40.595	15.698	32.204	49.052	45.366
20	14.722	42.416	41.328	15.548	32.221	49.179	46.658
21	14.731	42.750	41.484	15.540	32.187	49.164	46.894
22	14.722	42.962	41.539	15.665	32.230	49.120	47.171
23	14.722	42.939	41.514	15.631	32.221	49.162	47.286
24	14.667	43.059	41.632	15.515	32.187	49.146	47.340
25	14.703	43.076	41.547	15.465	32.144	49.018	47.437
26	14.676	43.187	41.775	15.590	32.238	49.043	47.570
27	14.722	43.094	41.741	15.673	32.247	49.103	47.534
28	14.749	43.119	41.716	15.650	32.238	49.111	47.481
29	14.658	42.733	41.630	15.631	32.230	49.077	47.048
30	14.667	42.373	41.168	15.631	32.221	49.189	46.605
31	14.685	41.969	40.932	15.656	32.210	49.129	46.136
32	14.776	41.983	40.957	15.648	32.204	49.137	45.962
33	14.694	41.772	41.033	15.614	32.247	49.171	45.906

Input and Pressure Data: Run 2, 3/14/95

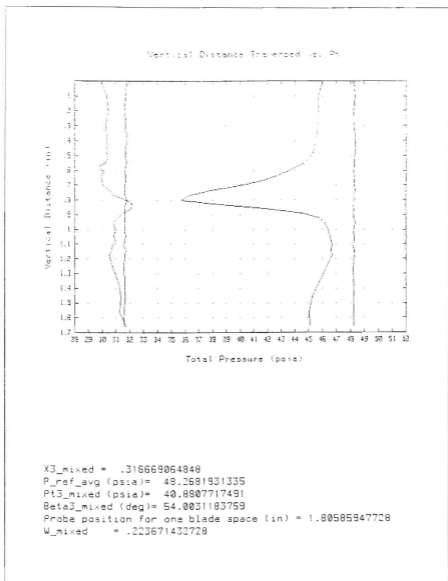


Pressure Distribution Plot and Flow Loss Results: Run 2, 3/14/95

Data Print Out for Exp # 1, Run # 12, File 2915031412
 Period between samples (sec): 1.003030303030
 Sample collection rate (Hz): 330
 Number of samples per point: 10
 Length of data run (sec): 33
 The scan type is: 3
 Number of scans/traverses: 33
 Atmospheric pressure is: 14.3071 psia
 Tunnel Pressure Ratio is: 2.09099402197

Scan	01	Port Number 24	25	28	30	31	32
1	14.748	42.025	39.778	15.257	31.750	48.244	45.997
2	14.793	42.025	39.744	15.207	31.725	48.328	45.714
3	14.748	41.991	39.795	15.224	31.690	48.212	45.928
4	14.784	41.922	39.753	15.174	31.716	48.279	45.970
5	14.775	41.985	39.801	15.224	31.769	48.328	45.546
6	14.793	41.775	39.391	15.207	31.742	48.372	45.306
7	14.802	41.630	39.204	15.249	31.725	48.312	45.053
8	14.820	41.329	39.358	15.241	31.750	48.312	44.695
9	14.793	40.813	38.593	15.216	31.716	48.259	44.190
10	14.775	40.306	37.957	15.291	31.673	48.252	43.437
11	14.820	39.825	37.296	15.232	31.733	48.304	42.604
12	14.839	39.819	36.503	15.216	31.725	48.312	41.559
13	14.721	37.632	35.471	15.349	31.673	48.259	39.910
14	14.811	36.152	34.542	15.241	31.639	48.355	37.818
15	14.829	34.957	33.915	15.216	31.682	48.235	36.275
16	14.820	34.631	34.001	15.191	31.750	48.304	35.717
17	14.783	36.359	35.547	15.282	31.716	48.133	37.842
18	14.793	38.896	38.064	15.232	31.673	48.244	41.754
19	14.802	40.804	39.797	15.257	31.673	48.261	44.598
20	14.802	41.707	40.504	15.232	31.665	48.244	45.785
21	14.811	41.956	40.673	15.249	31.690	48.355	46.166
22	14.775	42.137	40.900	15.249	31.690	48.287	46.325
23	14.748	42.300	40.908	15.232	31.665	48.218	46.449
24	14.775	42.309	40.918	15.199	31.707	48.269	46.538
25	14.730	42.420	41.019	15.232	31.656	48.269	46.653
26	14.730	42.377	41.002	15.349	31.613	48.281	46.679
27	14.811	42.386	40.326	15.224	31.707	48.279	46.644
28	14.775	42.317	40.968	15.249	31.656	48.295	46.679
29	14.721	41.991	40.749	15.257	31.622	48.158	46.236
30	14.775	41.707	40.454	15.257	31.656	48.244	45.740
31	14.802	41.260	40.226	15.224	31.647	48.219	45.236
32	14.766	41.045	40.082	15.249	31.630	48.218	45.032
33	14.739	40.985	40.470	15.216	31.613	48.252	45.112

Input and Pressure Data: Run 3, 3/14/95

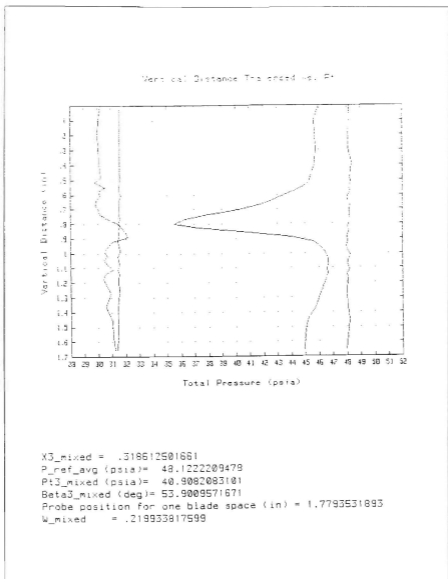


Pressure Distribution Plot and Flow Loss Results: Run 3, 3/14/95

Data Print Out for Test 4, Run # 1, File # 150307
 Period between samples (sec) : 0.010101010101
 Sample collection rate (Hz) : 100
 Number of samples per point : 10
 Length of data run (sec) : 33
 Time scan type (s) : 0
 Number of scans/traverses(s) : 10
 Atmospheric pressure (psi) : 14.31 psia
 Tunnel Pressure Ratio (s) : 2.06629969899

Scan	Port Number						
	01	24	25	29	30	31	32
1	14.302	40.019	39.940	15.300	31.515	48.194	46.007
2	14.775	41.953	39.861	15.325	31.538	48.151	45.589
3	14.320	41.919	39.895	15.275	31.506	48.143	45.715
4	14.938	42.013	39.712	15.333	31.529	48.135	45.760
5	14.794	42.029	39.679	15.342	31.532	48.121	45.742
6	14.311	41.925	39.425	15.342	31.515	48.229	45.598
7	14.783	41.586	39.231	15.292	31.589	48.279	45.240
8	14.329	41.589	38.927	15.325	31.521	48.126	44.790
9	14.794	40.385	38.471	15.322	31.564	48.228	44.190
10	14.820	40.320	37.813	15.325	31.549	48.041	43.344
11	14.775	39.879	37.247	15.317	31.555	48.094	42.612
12	14.775	38.882	36.530	15.292	31.538	48.228	41.606
13	14.793	37.849	35.652	15.350	31.555	48.168	40.188
14	14.793	36.199	34.437	15.350	31.538	48.185	37.971
15	14.793	34.856	33.737	15.333	31.589	48.202	36.257
16	14.784	34.511	33.661	15.300	31.512	48.118	35.472
17	14.784	35.632	35.070	15.342	31.521	48.058	37.291
18	14.775	38.157	37.593	15.350	31.469	48.125	40.918
19	14.820	40.457	39.594	15.292	31.469	47.991	43.979
20	14.856	41.637	40.244	15.350	31.410	48.084	45.601
21	14.757	41.791	40.699	15.242	31.572	47.948	46.077
22	14.847	42.090	40.784	15.250	31.581	48.084	46.421
23	14.739	42.295	40.919	15.442	31.461	48.312	46.579
24	14.802	42.278	40.977	15.317	31.504	48.041	46.606
25	14.739	42.347	40.951	15.292	31.529	48.057	46.641
26	14.739	42.398	41.012	15.400	31.452	48.177	46.597
27	14.793	42.270	40.910	15.259	31.529	48.007	46.606
28	14.775	42.210	40.834	15.325	31.495	48.050	46.544
29	14.874	41.929	40.699	15.375	31.521	48.016	46.121
30	14.811	41.671	40.269	15.383	31.439	48.067	45.759
31	14.757	41.107	40.066	15.317	31.419	48.160	45.125
32	14.302	40.945	39.999	15.342	31.444	48.084	44.958
33	14.775	40.851	40.100	15.292	31.393	47.931	44.922

Input and Pressure Data: Run 4, 3/27/95



Pressure Distribution Plot and Flow Loss Results: Run 4, 3/27/95

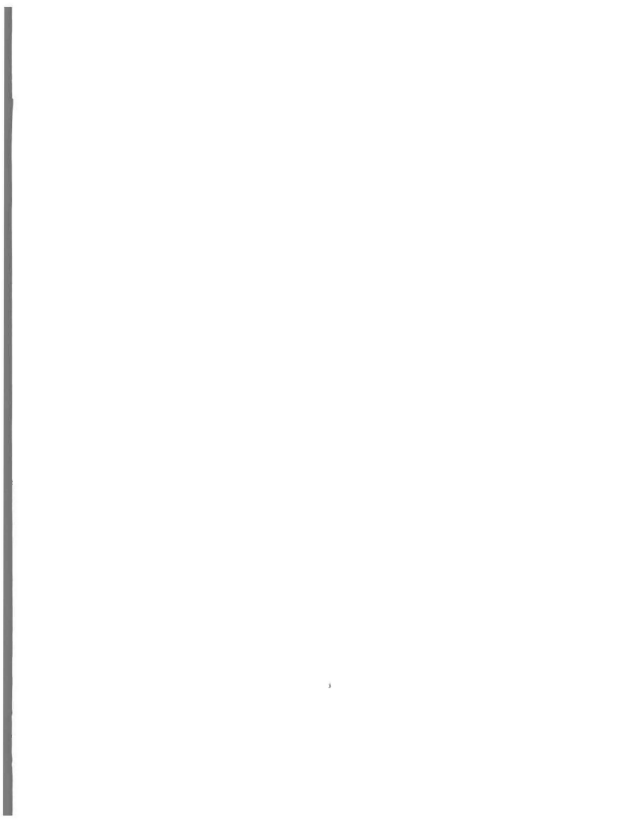
LIST OF REFERENCES

1. United Technologies Research Center Report R90-957946, "Transonic Fan Shock-Boundary Layer Separation Control," April 1990.
2. United Technologies Research Center Report R93-957946, "Transonic Fan Shock-Boundary Layer Separation Control: Final Report," December 1993.
3. McCormick, D. C., "Shock-Boundary Layer Interaction Control with Low-Profile Vortex Generators and Passive Cavity," AIAA Paper 92-0064, January 1992.
4. Demo, Jr., W. J., Cascade wind Tunnel for Transonic Compressor Blading Studies, M.S.A.E. Thesis, Naval Postgraduate School, Monterey, California, June 1978.
5. Hegland, M. G., Investigation of a Mach 1.4 Compressor Cascade with Variable Back Pressure Using Flow Visualization, M.S.A.E. Thesis, Naval Postgraduate School, Monterey, California, 1986.
6. Collins, C. C., Preliminary Investigation of the Shock-Boundary Layer Interaction in a Simulated Fan Passage, M.S.A.E. Thesis, Naval Postgraduate School, Monterey, California, March 1991.
7. Golden, W. L., Static Pressure Measurements of the Shock-Boundary Layer Interaction in a Simulated Fan Passage, M.S.A.E. Thesis, Naval Postgraduate School, Monterey, California, March 1992.
8. Myre, D. D., Model Fan Passage Flow Simulation, M.S.A.E. Thesis, Naval Postgraduate School, Monterey, California, December 1992.
9. Tapp, E. A., Development of a Cascade Simulation of a Fan Passage Flow, M.S.A.E. Thesis, Naval Postgraduate School, Monterey, California, December 1993.
10. Austin, J. G., Mach Number, Flow Angle, and Loss Measurements Downstream of a Transonic Fan-Blade Cascade, M.S.A.E. Thesis, Naval Postgraduate School, Monterey, California, March 1994.
11. Wendland, R. A., Upgrade and Extension of the Data Acquisition System for Propulsion and Gas Dynamic Laboratories, M.S.A.E. Thesis, Naval Postgraduate School, Monterey, California, June 1992.
12. HP 3455A Digital Voltmeter, "Operating Manual," Hewlett Packard Company, 1984.
13. HP 3497A Data Acquisition and Control Unit, "Operating, Programming and Configuration Manual," Hewlett Packard Company, 1982.

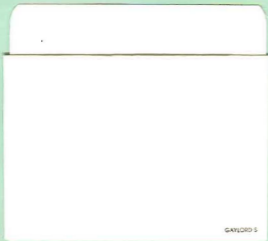
14. NF90 Stepping Motor Controller, "NF90 Series User's Guide One, Two and Three Axis Stepping Motor Controller/Drivers," VELMEX Incorporated, March 1991.
15. UniSlide Motor Driven Assembly, "Installation and Maintenance Instructions," VELMEX Incorporated, August 1990.
16. Armstrong, J., Near Stall Measurements in a CD Compressor Cascade with Exploratory Leading Edge Flow Control, M.S.A.E. Thesis, Naval Postgraduate School, Monterey, California, June 1990.
17. Wheeler, G. O., "Means for Maintaining Attached Flow of a Flowing Medium," United States Patent 4,455,045, June 1984.
18. McCormick, D. C., Private Communication.
19. Villarreal, Reynaldo and Tofanel, Sergiu, "Investigation of Vortex Generator Drag," (unpublished laboratory report), MIT, May 1992.
20. Suder, K. L., Chima, R. V., Strazisar, A. J. and Roberts, W. B., "The Effect of Adding Roughness and Thickness to a Transonic Axial Compressor Rotor," ASME Paper 94-GT-339, June 1994.

INITIAL DISTRIBUTION LIST

- | | | |
|----|---|--------------|
| 1. | Defense Technical Information Center
Cameron Station
Alexandria, Virginia 22304-6145 | 2 |
| 2. | Dudley Knox Library, Code 52
Naval Postgraduate School
Monterey, California 93943-5101 | 2 |
| 3. | Department of Aeronautics and Astronautics
Naval Postgraduate School
699 Dyer Road, Room 137
Monterey, California 93943-5106
ATTN: Chairman, Code AA
ATTN: Professor R. P. Shreeve, Code AA/SF
ATTN: Professor G. V. Hobson, Code AA/HG | 1
10
1 |
| 4. | Commander
Naval Air Systems Command
Code AIR 4.4.T
1421 Jefferson Davis Highway
Arlington, Virginia 22243 | 1 |
| 5. | Naval Air Warfare Center
Aircraft Division
Code AIR 4.4.3.1 [S. McAdams]
Propulsion and Power Engineering, Bldg. 106
Patuxent River, Maryland 20670-5304 | 1 |
| 6. | Dr. Duane C. McCormick
United Technologies Research Center
411 Silver Lane, MS 129-17
East Hartford, Connecticut 06108 | 1 |
| 7. | Mr. Peter M. Gamerding
P.O. Box 4753
Carmel, California 93921-4753 | 2 |



DUDLEY KNOX LIBRARY
NAVAL POSTGRADUATE SCHOOL
MONTEREY CA 93943-5101



GAYLORD 5

DUDLEY KNOX LIBRARY



3 2768 00307983 1